JPET Fast Forward. Published on December 15, 2015 as DOI: 10.1124/jpet.115.229864
This article has not been copyedited and formatted. The final version may differ from this version.

1. Title Page

The Role of Anti-drug Antibodies in the Pharmacokinetics, Disposition, Target Engagement, and Efficacy of a GITR Agonist Monoclonal Antibody in Mice

Nicholas D Brunn, Smita Mauze, Danling Gu, Derek Wiswell, Roanna Ueda, Douglas Hodges, Amy M Beebe, Shuli Zhang, and Enrique Escandón

Biologics DMPK & Disposition (N.B., D.W., D.H., E.E.), Immuno-oncology (S.M., D.G., R.U., A.B.), and Bioanalytics Department (S.Z.), Merck Research Laboratories, Merck & Co. Inc. Palo Alto, California

Downloaded from jpet.aspetjournals.org at ASPET Journals on April 16, 2024

Proprietary

JPET Fast Forward. Published on December 15, 2015 as DOI: 10.1124/jpet.115.229864
This article has not been copyedited and formatted. The final version may differ from this version.

2. Running Title Page

a) Running Title: The Impact of Anti-DTA-1 Antibodies on DTA-1 Pharmacology

b) Corresponding Author: Dr. Enrique Escandon, 901. S. California Avenue Palo Alto, CA 94304-1104, 1-650-496-1116, Enrique.escandon@merck.com

c) Number of: Text pages: 36

Number of: Tables: 2

Number of: Figures: 11

Number of: References: 59

Number of words in…

Abstract: 245

Introduction: 547

Discussion: 1209

d) Nonstandard abbreviations:

ADA, anti-drug antibodies; BSA, bovine serum albumin; CTLA-4, cytotoxic T-lymphocyte-associated protein 4; DMSO, dimethyl sulfoxide; DOL, degree of labeling; FACS, fluorescence activated cell sorting; FBS, fetal bovine serum; ELISA, enzyme-linked immunosorbent assay; FELA, fluorescence emission-linked assay; GITR, glucocorticoid-induced tumor necrosis factor receptor related protein; HMW, high molecular weight; HPLC, high performance liquid chromatography; IC, immune complex; IGG, immunoglobulin G; IMR, immunoregulatory receptors; MFI, Median Fluorescence Intensity; PBS, phosphate buffered saline; PD-1, Programmed cell death protein 1; PK, pharmacokinetic; SEC, size exclusion chromatography; TNF, tumor necrosis factor

e) Recommended section assignment: Inflamation, Immunopharmacology, and Asthma

Downloaded from jpet.aspetjournals.org at ASPET Journals on April 16, 2024

Pr Proprietary

JPET Fast Forward. Published on December 15, 2015 as DOI: 10.1124/jpet.115.229864
This article has not been copyedited and formatted. The final version may differ from this version.

3. Abstract

Administration of biologics to enhance T-cell function is part of a rapidly growing field of cancer immunotherapy demonstrated by the unprecedented clinical success of several immunoregulatory receptor targeting antibodies. While these biological agents confer significant antitumor activity through targeted immune response modulation, they can also elicit broad immune responses potentially including the production of anti-drug antibodies (ADAs). DTA-1, an agonist monoclonal antibody against the glucocorticoid-induced TNF receptor-related protein (GITR) is a highly effective antitumor treatment in preclinical models. We demonstrate that repeated dosing with murinized DTA-1 (mDTA-1) generates ADAs with corresponding reductions in drug exposure and engagement of GITR on circulating $CD3^+CD4^+$ T cells, due to rapid hepatic drug uptake and catabolism. Mice implanted with tumors after induction of preexisting mDTA-1 ADA show no antitumor efficacy when given 3 mg/kg mDTA-1, an efficacious dose in naïve mice. Nonetheless, increasing mDTA-1 treatment to 30mg/kg in ADA positive mice restores mDTA-1 exposure and GITR engagement on circulating $CD3^+$ $CD4^+$ T cells, thereby partially restoring antitumor efficacy. Formation of anti-mDTA-1 antibodies and changes in drug exposure and disposition does not occur in $GITR^{-/-}$ mice, consistent with a role for GITR agonism in humoral immunity. Finally, the administration of muDX400, a murinized monoclonal antibody against the checkpoint inhibitor PD-1, dosed alone or combined with mDTA-1 did not result in reduced muDX400 exposure, nor change the nature of the anti-mDTA-1 response. This indicates that anti-GITR immunogenicity may not necessarily impact the pharmacology of co-administered monoclonal antibodies, supporting combination immunomodulatory strategies.

Downloaded from jpet.aspetjournals.org at ASPET Journals on April 16, 2024

Pr Proprietary

JPET Fast Forward. Published on December 15, 2015 as DOI: 10.1124/jpet.115.229864
This article has not been copyedited and formatted. The final version may differ from this version.

5. Introduction

Due to their long half-life, high specificity, and excellent therapeutic window, antibodies and antibody-based biologics constitute one of the more successful classes of recently developed products in the biotechnology industry (Beck et al. 2010, Reichert. et al., 2011). Significant focus has recently been directed towards immune system modulating biologics, with monoclonal antibodies directed against immune checkpoint receptors including Programmed Cell Death Protein 1 (PD-1) and Cytotoxic T-Lymphocyte-Associated Protein 4 (CTLA-4) showing favorable pharmacokinetics and significant survival benefit in mouse models and in clinical studies (Hodi et al. 2010, Robert et al. 2011, Hamid et.al. 2013, Topalian et al. 2012, Wolchok et al. 2013, Melero et al. 2007, Peggs et al. 2009, Page et al. 2014).

In addition to targeting immune checkpoint inhibitors, biologics targeting members of the tumor necrosis factor receptor (TNFR) superfamily are emerging as an additional avenue of cancer immunotherapy (Murata et.al. 2006, Sugamura et al. 2004, Waldmann et al. 2006, Watts et al. 2005, Croft et al. 2013*).* One of these targets is the glucocorticoid-induced TNFR-related protein (GITR), a T cell costimulatory receptor (Ronchetti et al. 2004, Schaer et al. 2013). It has been shown that GITR can regulate immunity by potentiating $CD4^+$ and $CD8^+$ effector T cell function while modulating regulatory T cells (Nocentini et al. 2005, Nishikawa et al. 2008, Kohm et al. 2004, Kanamaru et al. 2004, Tone et al. 2003). In tumor bearing mice, treatment with the GITR agonist monoclonal antibody mDTA-1 has been shown to increase intratumoral effector T cell function and decrease regulatory T cell stability, culminating in effective tumor regression (Coe et al. 2010, Cohen et al. 2006, 2010, Zhou et al. 2007).

While modulation of costimulatory pathways have shown great preclinical potential as immunotherapies, immune related adverse events ranging from hyper-costimulation, to cytokine dysregulation and immunogenicity have been observed (Clarke et al. 2010, Reuben et al. 2006, Suntharalingam et al. 2006, Brennan et al. 2010, Chirino et al. 2004, Murphy et al. 2014). Ultimately, the administration of any biologic has the potential to generate anti-drug antibodies (Badylak et al. 2008, Shankar et al., 2006, 2007, Pepinsky et al. 2001). Although the degree of immunogenicity against a particular therapeutic is typically based on inherent properties of the molecule being administered (Badylak et al. 2008, Chirino et al. 2004, De Groot et al. 2007, 2009); other factors such a dose, dose regimen, route of administration and disease status of the host could also play a significant role. The

Pr Proprietary

Downloaded from jpet.aspetjournals.org at ASPET Journals on April 16, 2024

JPET Fast Forward. Published on December 15, 2015 as DOI: 10.1124/jpet.115.229864
This article has not been copyedited and formatted. The final version may differ from this version.

presence of anti-drug-antibodies can dramatically alter the PK and PD properties of administered biologics due to immune-complex formation changes in disposition and in the case of neutralizing antibodies by modulating biological activity. Furthermore, due to their unique mechanism of action, biologics targeting immunoregulatory receptors may enhance not only specific anti-tumor immune responses, but also lead to nonspecific immunologic activation and the possible emergence of immune disorders (Brennan et al. 2010, Kohm et al. 2004). Therefore a complete characterization of the biological responses to potent immunomodulatory drugs following extended exposure is critical to better predicting their therapeutic window. Here we describe for the first time the dramatic GITR-mediated pharmacokinetic and pharmacological changes that follow repeated treatment with a murinized IgG2a version of the anti-GITR agonist monoclonal antibody DTA-1 (mDTA-1) when dosed alone or in combination with the PD-1 antagonist antibody muDX400.

Downloaded from jpet.aspetjournals.org at ASPET Journals on April 16, 2024

Proprietary

JPET Fast Forward. Published on December 15, 2015 as DOI: 10.1124/jpet.115.229864
This article has not been copyedited and formatted. The final version may differ from this version.

6. Materials and Methods

All mouse procedures were performed in accordance with the Institutional Animal Care and Use Committee at Merck, and housed in a facility approved by the American Association for Assessment and Accreditation of Laboratory Animal Care (AAALAC), and maintained under a protocol in accordance with the guidelines of the AAALAC.

Mice, tumor cell lines, and anti-tumor efficacy experiments

Unless otherwise stated, all dosing was conducted as a subcutaneous bolus dose given in the upper scruff on the back of neck. In tumor growth experiments, care was given to dose as far away from the tumor as possible. C57BL/6J mice were obtained from the Jackson Laboratory (Bar Harbor, ME, USA), and BALB/c mice were obtained from the Taconic (Hudson, NY). Mice were approximately 8-14 weeks of age with body weights ranging from 20-25 grams. In the anti-tumor efficacy experiments, BALB/c mice were inoculated subcutaneously with 3.0×10^5 CT26 murine colon carcinoma cells (ATCC, Manassas, VA), and C57BL/6J mice were inoculated subcutaneously with 1.0×10^6 MC38 murine colon carcinoma cells (National Cancer Institute, USA). Cells were injected in 100 microliters volume. For antitumor efficacy experiments, upon achieving a tumor burden of approximately $100mm^3$, as gauged by electronic calipers, mice were given a single subcutaneous injection of 3 or 30mg/kg mDTA-1 or IgG2a isotype control. Additional cohorts of naïve and ADA positive mice were given three separate subcutaneous doses of 3 mg/kg mDTA-1 (q7d x 3). Tumor growth was monitored twice per week for approximately 3 weeks, at which point the animals were euthanized. Tumor length and width were measured using the electronic caliper and tumor volume determined using the following formula: Volume (mm^3) = 0.5 × length × $width^2$, where length is the longer dimension.

Monoclonal antibodies:

Murinized DTA-1 IgG2a (anti-GITR), muDX400 IgG1 D265A (anti-PD-1), and mouse anti-VP2 IgG2a (isotype control) were produced, purified, and characterized by the Protein Sciences Group at Merck & Co. Inc. Palo Alto, CA. FITC- Anti-mouse CD3, eFluor 450 anti-mouse CD4 and Alexa Fluor ® 488-Anti-F4/80 were purchased from BD Biosciences (San Jose, CA).

Pr Proprietary

Downloaded from jpet.aspetjournals.org at ASPET Journals on April 16, 2024

JPET Fast Forward. Published on December 15, 2015 as DOI: 10.1124/jpet.115.229864
This article has not been copyedited and formatted. The final version may differ from this version.

Fluorescent labeling:

DyLight 650 NHS ester labeling kits (Life Technologies) were used to conjugate an N-hydroxysuccinimide ester fluorophore (ex/em of 646/674) to label the experimental proteins of interest. Prior to labeling, antibodies were dialyzed into 50mM sodium borate (Life Technologies) utilizing a 10-kDa molecular weight cutoff Slide-A-Lizer dialysis cassette (Life Technologies). Each reaction contained protein at a final concentration of approximately 2 mg/ml. The conjugation was initiated by combining the protein with the DMSO-dissolved dye, and incubating for 1 hour at room temperature. Unreacted DyLight 650 was removed using a Thermo Scientific Pierce Dye Removal Column according to manufacturer protocols. If needed, protein samples were concentrated with a 30-kDa MW cutoff Amicon ultracentrifugation filter unit (EMD Millipore Corp. Billerica, MA), and sterile filtered using a 0.22-µm Millex syringe filter (EMD Millipore). Labeled antibodies were characterized using a NanoDrop UV-Vis spectrophotometer (Thermo Fisher Scientific, Waltham, MA) to determine the protein concentration and degree of labeling (DOL) as dye/protein (mole/mole) ratio. The integrity of the labeled antibodies was additionally assessed by SEC-HPLC, and by extended incubation in PBS and wild type BALB/c mouse plasma (data not shown). All reagents were analyzed for purity and activity by several methods prior to administration (data not shown). All DyLight-650 labeled antibodies had an average degree of labeling of 2.1 dye molecules per antibody.

Pretreatment of BALB/c mice

For generating ADA positive mice, either two or three doses of indicated antibody were administered with 7 day or 14 day intervals. Previous experiments have shown no measurable differences between ADA titers of animals pretreated with 2, 3, or 4 doses of mDTA-1. All antibodies were unlabeled and administered by subcutaneous injection in either 100 or 200 µL of sterile phosphate buffered saline (PBS) or appropriate buffer. In pharmacokinetic experiments, mice were dosed twice, 7 days apart, with either 3 milligram per kilogram (mg/kg) single agent, or 1.5 mg/kg of each agent in combination in 100µL PBS. For tumor model experiments, mice were dosed three times, 14 days apart, with 3 mg/kg mDTA-1. In all cohorts, there was a 10-20 day washout period prior to experimentation to allow for the removal of unlabeled mDTA-1 or muDX400 (confirmed by ELISA).

Downloaded from jpet.aspetjournals.org at ASPET Journals on April 16, 2024

Pr Proprietary

JPET Fast Forward. Published on December 15, 2015 as DOI: 10.1124/jpet.115.229864
This article has not been copyedited and formatted. The final version may differ from this version.

Blood and Tissue Collection

Animals were euthanized with carbon dioxide followed by terminal cardiac puncture. Blood was collected into EDTA-K_2 CapiJect micro collection tubes (Terumo Medical Corporation, Somerset, NJ) and placed on ice. Plasma was separated from whole blood via centrifugation for 6 minutes at 6000 x g at 4ºC, and stored at -80ºC. Likewise, whole blood samples were aliquoted into polypropylene vials (Corning Glassworks, Corning, NY) and stored at -80ºC. For tissue lysates, organ samples were collected and immediately placed into 2ml Precellys Lysing Tubes (Bertin Technologies, Rockville, MD) and placed into dry ice. Upon partial thawing, a 1:10 dilution of dPBS containing 1% Triton X-100 (MP Biomedicals, Solon, OH) and 1x Halt Protease Inhibitor single-use cocktail (Thermo Scientific) was added to the samples. Then tissue slurries were produced using a Precellys Evolution homogenizer. The slurry was centrifuged (10,000 x g at 4ºC for 10 minutes) and the tissue lysate supernatants were collected and either processed immediately, or stored at -80ºC until analysis.

Size exclusion chromatography-high performance liquid chromatography analysis

Samples were applied onto a BioSep-SEC-S 3000 column with an inline Security Guard filter (Phenomenex, Torrance, CA) and analyzed using an Agilent 1200 HPLC system, utilizing an integrated UV and fluorescence detector (Agilent Technologies, Santa Clara, CA; Hamamatsu Corperation, Bridgewater, NJ) respectively. The size exclusion protocol utilized a 15-minute isocratic run with Dulbecco's PBS buffer (HyClone, GE Life Sciences, Little Chalfont, UK) as the mobile phase, and was run at a constant flow rate of 1 $ml*min^{-1}$ and kept at room temperature. The effluent was monitored continuously by optic observation at 280nm and by the net fluorescence intensity at excitation wavelength of 646nm, and emission of 674nm. For mDTA-1 incubation experiments, plasma from naïve and mDTA-1 pretreated mice (after a 15 day washout period) was collected as previously described. Defined quantities of mDTA-1 or an IgG2a isotype control (50, 100, or 250 µg/mL) was spiked into 20 µL of neat plasma, incubated for 15 minutes at 37ºC, and applied to the BioSep-SEC-S 3000 column. The analysis and data collection was performed using the Agilent Technologies' ChemStation software, as well as EXCEL (Microsoft Corporation, Seattle, WA), and GraphPad (GraphPad Software, Inc, La Jolla, CA). The column performance was assessed prior to and following each batch of samples by running 20 microliters of a standard set of molecular weight markers (Bio-Rad Laboratories, Hercules, CA).

Pr Proprietary

Downloaded from jpet.aspetjournals.org at ASPET Journals on April 16, 2024

JPET Fast Forward. Published on December 15, 2015 as DOI: 10.1124/jpet.115.229864
This article has not been copyedited and formatted. The final version may differ from this version.

Fluorescence Emission Linked Assay (FELA)

Net fluorescence intensity was quantified utilizing a Promega Glowmax plate reader (Promega, Madison, WI) equipped with a fluorescence optical filter with excitation/emission wavelengths of 625/660-720. Concentrations of fluorophore labeled protein were calculated by generating individual calibration curves in naïve BALB/c liver tissue, whole blood, and plasma for each DyLight 650 labeled test article. These calibration curves were analyzed using low fluorescence background black 96-well polystyrene assay plates (Corning), and blank tissue lysates, blood, and plasma were used for background corrections. A linear correlation function was fitted to the data using "best fit" parameters (EXCEL). Concentrations of DyLight labeled test articles were calculated as microgram equivalents per gram of wet tissue. Subsequent tissue/blood ratios were calculated by comparing the quantified concentrations of the test articles in the respective tissue types versus the concentration in blood at the indicated time point. Ratios were calculated using EXCEL.

Capillary Fluorescent Electrophoresis Analysis (CAFÉ)

Tissue lysates were analyzed using a Caliper Lifesciences LabChip GX II microfluidic capillary electrophoresis apparatus (Perkin Elmer, Hopkinton, MA) according to the manufacturer's protocol. Briefly, the tissue lysates (previously diluted 1:10 in tissue lysate buffer) were diluted an additional 2-10 fold in the Caliper sample buffer, denatured at 75ºC for 5 minutes, centrifuged at 2,000 x g for 2 minutes, and then run. Electropherograms were generated by LabChip GXII Touch software.

Tissue Distribution and Pharmacokinetic Analysis

For pharmacokinetic analysis and biodistribution of mDTA-1 and muDX400 antibodies, mice were separately given a single subcutaneous bolus dose of either 5mg/kg or 30mg/kg DyLight 650 labeled mDTA-1 or muDX400. The animals were sacrificed at the previously indicated time points of 2, 4, 6, 8, 24, and 96 hours (5 mg/kg) or 4, 8, 16, 48, and 96 hours (30 mg/kg). The concentrations of test articles in serum, whole blood, and selected tissues was quantified by a fluorescence emission-linked assay (FELA), whose lower detection limits are approximately 5ng/ml for DyLight 650 labeled experimental proteins. Pharmacokinetic parameters were calculated in WinNonlin (Pharsight, Mountain View, CA) using noncompartmental methods on the concentration-time data quantified in the FELA assay. The

Downloaded from jpet.aspetjournals.org at ASPET Journals on April 16, 2024

Pr Proprietary

JPET Fast Forward. Published on December 15, 2015 as DOI: 10.1124/jpet.115.229864
This article has not been copyedited and formatted. The final version may differ from this version.

concentration-time data for all antibodies was plotted using GraphPad Prism 6, and are presented with their corresponding S.D.

Fluorescent analysis of immune complex uptake in mouse Kupffer cells

Naïve and mDTA-1 pretreated wild type BALB/c mice (previously inoculated with 3 mg/kg mDTA-1 q7d x 2) were injected subcutaneously with 30 mg/kg DyLight labeled mDTA-1 and Kupffer cells were enriched from liver associated cells as previously described (Li et al. 2014, Zeng et al. 2013). Briefly, 24 hours post-dose, mice were euthanized and underwent cardiac perfusion with 3 mL × min^{-1} PBS for 3 minutes. The livers were removed, minced, and collected in 30 mL RPMI media + 10% FBS + 0.1% collagenase IV, and subsequently incubated at 37ºC for 30 minutes. Kupffer cells were enriched from hepatocytes, non-parenchymal, and liver sinusoidal endothelial cells by gradient centrifugation. Heavy sediments were removed by centrifugation at 20 x g for 2 minutes and the pellet was discarded. Larger cells were removed by centrifugation at 50 x g for 3 minutes and the pellet was discarded. Cells were clarified by two alternating rounds of centrifugation of 50 x g for 3 minutes (discarding the pellet), and 300 x g for 3 minutes (discarding the supernatant) and always resuspended in 5 mL of RPMI media. On the final spin, cells were resuspended with 500µL RPMI media and incubated with 5µg/ml AlexaFluor 488-anti-F4/F80 antibody for 30 minutes at 4ºC. Cells were then plated directly atop microscopy slides and allowed to adhere for 2 hours. Non-adherent cells were removed by 3 washes with PBS. Cells were then visualized with an EVOS FL Cell Imaging System containing both the Green Fluorescent Protein (GFP), and Cy®5 Light Cubes. Images were acquired and overlaid utilizing the onboard EVOS FL software.

Anti-drug antibody detection and free-drug detection assays

Mice were pretreated with indicated antibody (3 mg/kg q7d x 3) and plasma samples collected as described previously. Six mice were used per time point. Plasma samples were then run on a Meso Scale Discovery (MSD) bridging immunogenicity assay. MSD plates were coated with 150 µL of Blocker A solution (5 g BSA (5%) in 100 mL DPBS) per well and stored at 4ºC overnight (or up to 4 days). A mixture of 1 µg/mL biotin-DTA-1 and 1ug/mL sulfo-DTA-1 were prepared in AD Buffer (0.5% BSA, 0.05% Tween 20, 0.25% 3-[(3-Cholamidopropyl) dimethylammonio]-1- propanesulfonate (CHAPS), 5mM EDTA, 0.35M NaCl, in PBS, pH7.4). 100 µL of DTA-1 mix from previous step was added to each well of the reaction plate (Corning cat#3605, non-binding surface). 35 µL of AD buffer was added to each well.15 µL of neat

Pr Proprietary

Downloaded from jpet.aspetjournals.org at ASPET Journals on April 16, 2024

JPET Fast Forward. Published on December 15, 2015 as DOI: 10.1124/jpet.115.229864
This article has not been copyedited and formatted. The final version may differ from this version.

sample plasma (or pooled BALB/c mouse serum for background wells) were added to each well, mixed and incubated on plate shaker at 300RPM for 2 hour at RT. Samples were washed, while MSD plates were blocked, 3 times with washing buffer (PBS with 0.5% Tween 20). 50 µL of the sample mixture from prior step was added to duplicate wells on the MSD read plate. Plate was incubated on shaker at 300RPM for 1 hour at RT. Plates were washed 3 times with washing buffer. 150 µL of MSD 1x Read Buffer T was added to each well and read on MSD instrument (SI-6000).

To determine the concentration of free mDTA-1 or muDX400 in circulation, a drug capture ELISA assay utilizing a recombinant mouse GITR or PD-1 protein as the capture antigen was used, followed by a horseradish peroxidase conjugated goat anti-mouse IgG as the detection antibody adhering to manufacturers protocols.

Flow cytometry and fluorescence assisted cell sorting

Mouse peripheral blood mononuclear cells (PBMC) were isolated from naïve or mDTA-1 pretreated (ADA positive) mice, 4 hours after a bolus dose of either 3, or 30 mg/kg labeled mDTA-1, or DyLight-650-mIgG2a isotype control. Briefly, whole blood was collected by terminal cardiac puncture and placed into EDTA treated collection tubes, and placed on ice. ACK red blood cell lysis buffer was added to whole blood at a 20 fold excess to lyse the RBCs according to the ACK Lysing Buffer Kit (Life Technologies) protocol. Samples were then centrifuged at 300 x g for 5 minutes at 4ºC. The supernatant was aspirated, and the isolated PBMCs were washed three times with ice-cold FACS buffer (Sigma-Aldrivh, St. Louis, MO, USA).

Cells from mice treated with DyLight-650 labeled mDTA-1 or isotype control were divided into two groups, one group was incubated with anti-CD3 and anti-CD4 (Experimental), the other group with anti-CD3, anti-CD4, and 5µg/ml DyLight 650-DTA-1 (Maximum MFI control). Cells were then washed three times in ice cold FACS buffer, followed by fluorescence-activated cell sorting, and analysis.

To establish the relative maximum and minimum MFIs of mDTA-1 GITR engagement, negative controls received no ex-vivo DTA-1 staining (Negative Control), and (Maximum) GITR engagement was accomplished through ex-vivo incubation with 5µg/ml DyLight 650-DTA-1 for 30 minutes. For labeled mDTA-1 or IgG2a isotype control, the “Percent GITR Binding” was calculated using the following formula:

% Bound= (Experimental MFI– Negative Control MFI) ÷ (Maximum MFI- Negative Control MFI) x 100

Pr Proprietary

Downloaded from jpet.aspetjournals.org at ASPET Journals on April 16, 2024

JPET Fast Forward. Published on December 15, 2015 as DOI: 10.1124/jpet.115.229864
This article has not been copyedited and formatted. The final version may differ from this version.

7. Results:

DyLight-650 labeled mDTA-1 antibody plasma concentration decreases rapidly over time in BALB/c mice previously treated with mDTA-1

Figure 1 shows the dramatic changes in the concentration time profiles of circulating mDTA-1 antibodies when administered to mice previously exposed to the drug relative to naive control mice. By 96 hours following subcutaneous (SC) administration the plasma concentrations in naïve mice were 28 and 161 ug/ml (5 and 30 mg/kg doses) versus 0.1 and 1.5 ug/ml respectively in mDTA-1 pretreated mice. PK parameters calculated from the concentration time profiles of both cohorts (**Table 1**) indicated that previous treatment with mDTA-1 resulted in a nonlinear reduction in exposure (AUClast); 24 fold (5mg/kg) and 7 fold (30 mg/kg). Corresponding changes in clearance and half-life were consistent with these reductions in AUClast in pretreated mice, and the PK parameters in naïve mice assume the elimination phase kinetics remain constant after the 96 hours collection point.

DTA-1 forms High Molecular Weight complexes in plasma from mDTA-1 pretreated mice

To gain a better understanding of the increased mDTA-1 elimination in pretreated versus naïve mice, mDTA-1 stability and potential protein interactions were characterized by fluorescent SEC-HPLC analysis. In the plasma of naïve mice, DyLight-650-mDTA-1 elutes as a single monomeric peak at all-time points (**Figure 2A**) consistent with intact IgG. No high molecular weight complexes, aggregates or catabolic products were observed. Whereas, in pretreated BALB/c mice, we observed the presence of high molecular weight (HMW) complexes with retention times of approximately 6 and 7 minutes corresponding to approximate molecular weights of 1MDa and 350kDa, respectively (**Figure 2B**). Consistent with the fast elimination of mDTA-1 in pretreated mice (**Figure 1B**), the DyLight-650 labeled mDTA-1 chromatographic signal was essentially depleted by 48 hours. The formation of HMW complexes in vivo is indicative of potential drug anti-drug immune complexes (ICs).

Furthermore a major shift was observed in the size exclusion profile of labeled mDTA-1 when incubated *in-vitro* in plasma from mice previously exposed to mDTA-1 changing from monomeric IgG to mostly HMW forms (**Figure 3**). This is in agreement with the presence of high ADAs levels and the rapid formation of drug-anti-drug immune complexes. As expected, no changes in the chromatographic profiles

Pr Proprietary

Downloaded from jpet.aspetjournals.org at ASPET Journals on April 16, 2024

JPET Fast Forward. Published on December 15, 2015 as DOI: 10.1124/jpet.115.229864
This article has not been copyedited and formatted. The final version may differ from this version.

were observed in naïve mouse plasma spiked with labeled mDTA-1, or plasma from pretreated mice spiked with an isotype control 650-labeled antibody. The relatively low level of mDTA-1 HMW complexes in circulation versus in spiked pretreated plasma (**Figures 2 B vs. Figure 3**) is consistent with a mechanism for rapid hepatic elimination of immune complexes (Lovdal et al. 2000, Ganesan et al. 2012).

Hepatic Uptake of 650-labeled DTA-1 in pretreated BALB/c mice

Total fluorescence profiles (microgram equivalents per milliliter of tissue lysate) of labeled mDTA-1 after subcutaneous injection of 30 mg/kg in naïve and pretreated BALB/c mice were measured over time in several organs and whole blood. A tissue/blood ratio greater than 1 is indicative of tissue uptake and accumulation. In naïve animals tissue/blood ratios remained below 0.5 (**Figure 4A**), with no evidence of drug accumulation in any organ analyzed (**Figure 4B**). In contrast, mice previously exposed to mDTA-1 experienced intense mDTA-1 organ uptake after dosing. Tissue/blood ratios in the liver, and to a lesser degree the kidneys, reached their highest values (~150 and 20 respectively) at 96 hours for the liver, and 48 hours for the kidney (**Figure 4C**). The total levels of 650-DTA-1 (µg / g tissue equivalents) were 10 fold higher by 24 hours post dose in the liver of pretreated mice relative to naïve animals (150 versus 17.5µg/ g) (**Figure 4B and 4D**). Overall, these results demonstrate that pretreatment with mDTA-1 dramatically changes the PK and disposition of fluorescent mDTA-1 resulting in dramatic liver uptake, atypical of normal IgGs.

Hepatic catabolism of DyLight 650-mDTA-1

To better characterize the dramatic changes in antibody exposure and liver uptake in pretreated mice, tissue lysates of naïve and pretreated BALB/c mice dosed with 30mg/kg fluorescent mDTA-1 were analyzed by capillary fluorescent electrophoresis (CAFÉ) to determine drug integrity (**Figure 5**). The major IgG band at approximately 150 kDa corresponds to intact mDTA-1 antibody and it is the main component in plasma from naïve mice (**Figure 5A**). Only trace amounts of degradation products were found in any organ analyzed including the liver (shown).

Conversely, consistent with the increased clearance, only low levels of intact mDTA-1 were present in plasma from BALB/c mice previously treated with mDTA-1 (**Figure 5B**). In the liver of these

Pr Proprietary

Downloaded from jpet.aspetjournals.org at ASPET Journals on April 16, 2024

JPET Fast Forward. Published on December 15, 2015 as DOI: 10.1124/jpet.115.229864
This article has not been copyedited and formatted. The final version may differ from this version.

mice the majority of the experimental antibody was catabolized as indicated by the abundance of small molecular weight degradation products denoted by the arrows. These results support the presence of circulating anti-drug antibodies in pretreated mice that upon retreatment form drug/anti-drug immune complexes (ICs). ICs then likely undergo rapid Fc gamma receptor mediated hepatic clearance and degradation as previously shown by others (Bogers et al. 1991, Lovdal et al. 2000, Ganesan et al. 2012). The efficient removal of potential ICs is in agreement with the low levels of circulating DTA-1 containing HMW complexes in pretreated mice as shown in **Figure 2B**.

Kupffer cell uptake of DyLight 650-mDTA-1

Kupffer cells are one of the major cell types involved in removal of ICs (Lovdal et al. 2000). To investigate their role in the increased hepatic catabolism of mDTA-1 in pretreated mice, KCs were isolated from livers of naïve and mDTA-1 pretreated animals and analyzed 24 hours after DyLight 650-mDTA-1 SC administration (**Figure 6**). Intense 650-mDTA-1 staining was prevalent in Kupffer cells from pretreated mice (red). No mDTA-1 fluorescence signal was observed in KCs from naïve mice suggesting that the increased elimination of mDTA-1 in pretreated mice was due in part by KC uptake of anti-mDTA-1/mDTA-1 immune complexes. Furthermore, ex-vivo staining with an Alexa Fluor-488 conjugated anti-F4/80 antibody, used to identify KCs (left panels), confirmed that all KCs were also positive for 650-mDTA-1 signal.

DTA-1 treatment elicits a target mediated anti-drug antibody response

To assess the relative levels of anti-drug antibodies and the potential role of the target (GITR) in anti-mDTA-1 immunogenicity and altered clearance, plasma samples from naïve or mDTA-1 pretreated wild type and GITR-/- C57BL/6 mice were collected at 3, 30, 60, and 90 days following a SC mDTA-1 dose of 3mg/kg mDTA-1.

Treatment with mDTA-1 in wild type mice led to a robust ADA response by day 30 following the most recent mDTA-1 administration and gradually declined, but remained positive through at least day 120. The ADA signal was over 10^5 fold higher than background levels observed in $GITR^{-/-}$ knockout mice

Pr Proprietary

Downloaded from jpet.aspetjournals.org at ASPET Journals on April 16, 2024

JPET Fast Forward. Published on December 15, 2015 as DOI: 10.1124/jpet.115.229864
This article has not been copyedited and formatted. The final version may differ from this version.

(**Figure 7A**). Likewise, there was no detectable mDTA-1 in plasma from wild type mice (LLOQ of 0.09 µg/mL) after 3 days post-dosing; whereas at days 3, 30, 60, and 90 the GITR$^{-/-}$ mice had average mDTA-1 concentrations of 31, 13, 3, and 0.6 µg/ml respectively (**Figure 7B**). These results clearly demonstrated that the agonistic antibody mDTA-1 critically requires the presence of the target (GITR) to induce a specific anti-drug response.

Restoration of DTA-1 antitumor efficacy in ADA positive mice

The impact of ADAs on mDTA-1 antitumor efficacy was evaluated in naïve and ADA positive BALB/c (**Figure 8 A, B**) and C57BL/6J mice (**Figure 8 C, D**) implanted with CT26 and MC38 syngeneic tumors, respectively. Mice with established tumors (average 100mm^3) were dosed SC with single or multiple doses of 3 mg/kg mDTA-1 at day 0 or at days 0, 7, and 14, respectively, or with a single 30 mg/kg dose. Average tumor volume was recorded every 3-4 days (**Figure 8A, C**) and the final tumor volumes were individually plotted and statistically analyzed (**Figure 8B and 8D)**. In naïve BALB/c and C57BL/6J mice, a 3 mg/kg single dose was sufficient to induce tumor regression in both the CT26 and MC38 tumor models. Efficacy was comparable between cohorts treated with a single dose of 3 or 30 mg/kg mDTA-1 or three weekly doses of 3 mg/kg. Conversely, in ADA positive mice, neither a single nor multiple doses of 3mg/kg mDTA-1 showed any antitumor activity. However, a single 30mg/kg dose of mDTA-1 did slow tumor progression in mice with pre-existing ADA, particularly in the MC38 model. The same response, although to a lesser degree, was observed in the CT26 model. The presence of anti-drug antibodies in these mice was confirmed by the MSD assay and SEC-HPLC (data not shown).

Efficient mDTA-1 target engagement in ADA positive mice can be achieved with a 10-fold increase in dose

The presence of anti-drug antibodies against mDTA-1 dramatically decreased tumoricidal activity. This was likely due in part to the enhanced elimination of the drug upon immune complex formation. In order to determine if the anti-drug antibodies would also neutralize mDTA-1 binding, we evaluated the effects of ADAs on mDTA-1 GITR engagement 4 hours after dosing using flow cytometry and fluorescence activated cell sorting.

Pr Proprietary

Downloaded from jpet.aspetjournals.org at ASPET Journals on April 16, 2024

JPET Fast Forward. Published on December 15, 2015 as DOI: 10.1124/jpet.115.229864
This article has not been copyedited and formatted. The final version may differ from this version.

A subcutaneous dose of 3 mg/kg of 650-labeled mDTA-1 engaged approximately 95% of circulating CD3+ CD4+ GITR cells in naïve mice in comparison to only ~5% in ADA positive mice (**Figure 9A**). Increasing the mDTA dose to 30 mg/kg restored the mDTA-1 target engagement to 91%. The MFI from the negative controls (no antibody) were comparable to the MFI observed from subcutaneous dosing of an IgG2a isotype control. Purified PBMCs were also visualized for mDTA-1 binding in all groups using a fluorescent microscope (**Figure 9B**). Abundant 650-celular staining was observed in both PBMCs from naïve mice dosed with 3 mg/kg and ADA positive mice dosed with 30 mg/kg. No fluorescence signal was detected in PBMC from ADA positive mice dosed with 3 mg/kg of mDTA-1 or with 3 or 30 mg/kg of isotype control antibody (data not shown). Flow cytometry analysis of circulating $CD3^+$ $CD4^+$ T cell populations in naïve and ADA positive mice (**Figure 9C**) demonstrated strong mDTA-1-GITR engagement in naïve mice dosed with 3 mg/kg. However, when ADA positive mice were given the same 3mg/kg 650-mDTA dose, no MFI changes were observed, consistent with decreased concentrations of available mDTA-1 in the circulation due either to fast ICs elimination and/or direct ADA neutralization of mDTA-1 binding. Importantly, mDTA-1 target engagement on peripheral blood CD4+CD3+ T cells was almost restored to naïve levels in ADA positive mice treated with 30 mg/kg.

Effect of pretreatment in the disposition of PD-1 antagonist muDX400 in BALB/c mice

Drug combinatorial approaches are rapidly becoming a hallmark of cancer treatment. Therefore a better understanding of potential pharmacological drug-drug interactions is critical to improving rational combination therapy design. To that end, *in vivo* pharmacokinetics and disposition were used to assess whether pretreatment with mDTA-1 dosed in combination with the PD-1 antagonist antibody muDX400 would further accelerate mDTA-1 disposition and/or immunogenicity (Hirsch et al. 2015, Pinheiro et al. 2015). In addition, we compared the effects of mDTA-1 versus muDX400 pretreatment, dosed alone or in combination, in the PK and disposition of muDX400.

Figure 10 shows muDX400 concentration time profiles in naïve, muDX400, and muDX400 + mDTA-1 pretreated BALB/c mice. Fluorescently labeled muDX400 concentration time profiles and pharmacokinetic parameters were indistinguishable irrespective of pretreatment combinations (Table 2). In contrast, there is a dramatic reduction in drug exposure for mDTA-1 in pretreated mDTA-1/muDX400

Pr Proprietary

Downloaded from jpet.aspetjournals.org at ASPET Journals on April 16, 2024

JPET Fast Forward. Published on December 15, 2015 as DOI: 10.1124/jpet.115.229864
This article has not been copyedited and formatted. The final version may differ from this version.

combo mice. Interestingly, the changes in mDTA-1 PK parameters in mice pretreated with mDTA-1 alone (Table 1) were similar to those pretreated in combination with muDX400. This suggests limited cross reactivity between these two immunoregulatory targets in the generation of an anti-drug response. Likewise, analysis of muDX400 disposition in muDX400 pretreated mice (**Figure 11 A, B**) and muDX400 + mDTA-1 pretreated mice (**Figure 11 C, D**) revealed that tissue:blood ratios of muDX400 remained below 0.5 in both cohorts at all collected time points (**Figure 11A, C**). This is indicative of negative tissue uptake or accumulation. Furthermore, distribution of muDX400 revealed no evidence of drug accumulation in any organ analyzed (**Figure 11 B, D**), demonstrating that muDX400 is highly stable in circulation with a non-specific organ disposition pattern typical of normal IgGs. In addition, plasma samples from a separate group of BALB/c mice pretreated q7d x2 with 3.0 mg/kg mDTA-1 (alone), 1.5 mg mDTA-1 + muDX400, or 3.0 mg/kg muDX400 (alone), were collected 21 days after the second dose, spiked with labeled muDX400, and examined by SEC-HPLC. The resulting chromatographs showed a single monomeric peak corresponding to intact IgG and no detectible HMW complexes (data not shown).

Downloaded from jpet.aspetjournals.org at ASPET Journals on April 16, 2024

Pr Proprietary

JPET Fast Forward. Published on December 15, 2015 as DOI: 10.1124/jpet.115.229864
This article has not been copyedited and formatted. The final version may differ from this version.

8. Discussion

This study characterized the impact of anti-drug antibodies on the pharmacology of the GITR agonist monoclonal antibody mDTA-1. We compared the pharmacokinetics, disposition, target engagement and antitumor efficacy of mDTA-1 in naïve and ADA positive mice. This study demonstrated that treatment with mDTA-1 in naïve wild type mice generated anti-mDTA-1 antibodies. Subsequent doses of mDTA-1 formed high molecular weight complexes in circulation, which led to hepatic deposition and drug elimination, thereby limiting drug exposure and reducing target engagement and antitumor efficacy of mDTA-1. Moreover we showed that this ADA response was GITR mediated, mDTA-1 specific, and did not alter the pharmacokinetics of a coadministered PD-1 antagonist, muDX400.

Interestingly, the lack of an ADA response against mDTA-1 in $GITR^{-/-}$ mice following repeated treatment strongly supports the hypothesis that direct agonistic engagement of GITR by mDTA-1 is responsible for the immunogenicity of the mDTA-1 molecule in wild type mice, as opposed to an unusually strong immunogenicity of the molecule itself. An investigation into this target mediated ADA mechanism might clarify whether mDTA-1 engagement of GITR on T cells or B cells (Zhou et al. 2010) is potentiating mDTA-1 immunogenicity.

The pharmacokinetics, disposition, and target engagement of biotherapeutics are typically evaluated through the use of either radioactively labeled molecules (Rojas et al. 2005, Kelly et al. 2013), fluorescently labeled molecules (Alvarez et al. 2012), or anti-drug assays (Bourdage et al. 2007, Kelly et al. 2013). In our study of mDTA-1 in naïve and ADA positive mice, we utilized fluorescent labeling of the mDTA-1 and muDX400 monoclonal antibodies to follow their fate *in vivo* at relevant pharmacological doses. Direct quantitation of labeled antibodies circumvents potential assay interference issues when assessing drug levels in the presence of anti-drug antibodies. SEC-HPLC analysis of mDTA-1 from plasma of ADA positive mice dosed or incubated with fluorescently labeled mDTA-1 reveal the presence of HMW complexes consistent with the presence of anti-mDTA-1/mDTA-1 immune complexes (Rojas et al. 2005, Lovdal et al. 2000, Ganesan et al. 2012). The relatively low concentration of ICs detected in blood by this method in ADA positive mice treated with 650-labeled DTA-1 versus the total conversion to HMW complexes formed by spiking 650-mDTA-1 *ex-vivo* in plasma from ADA positive mice suggests

Pr Proprietary

Downloaded from jpet.aspetjournals.org at ASPET Journals on April 16, 2024

JPET Fast Forward. Published on December 15, 2015 as DOI: 10.1124/jpet.115.229864
This article has not been copyedited and formatted. The final version may differ from this version.

that ICs were efficiently removed from the circulation. The non-linear reduction in DTA-1 exposure observed in pretreated animals dosed with 5 mg/kg versus 30 mg/kg suggests saturation of IC formation or a plateau in the elimination capacity of DTA-1/anti-DTA-1 immune complexes by the reticuloendothelial system. To ascertain the clearance mechanisms of mDTA-1 ICs in BALB/c mice, we conducted various tissue distribution analyses of DyLight 650-mDTA-1 administered to naïve and ADA positive cohorts. Our results suggested that following administration to mice with a preexisting ADA response against mDTA-1, the anti-drug antibodies bound to and formed ICs with mDTA-1. These ICs were then rapidly cleared through hepatic uptake, at least partially by Kupffer cells, followed by catabolism, and subsequent elimination. While this is consistent with previous studies (Loval et al. 2000, Ganesan et al. 2012) it does not preclude the possibility of IC uptake by other liver associated cells, such as liver sinusoidal endothelial cells, which in our studies showed sporadic 650-mDTA-1 staining (data not shown). Additionally, the renal uptake observed in ADA positive mice may be partially due to the excretion of free fluoroprobe in circulation resulting from ADA related drug processing (Nlend et al. 2014).

We demonstrated that while single dose and multiple dose regimens of 3 mg/kg mDTA-1 provided equivalent antitumor efficacy in naïve mice, neither was sufficient to achieve antitumor efficacy in mice with preexisting ADA. This revealed that mDTA-1 antitumor efficacy was ablated by the anti-mDTA-1 antibody response. Furthermore, we showed that in ADA positive mice, a 3 mg/kg mDTA-1 dose was insufficient to engage GITR on circulating $CD3^+$ $CD4^+$ T cells. This lack of target engagement was likely responsible for the diminished antitumor efficacy of mDTA-1 in ADA positive mice. When the mDTA-1 dose in ADA positive mice was increased to 30 mg/kg, GITR engagement on circulating $CD3^+$ $CD4^+$ T cells was comparable to that of naïve mice dosed with 3 mg/kg. Anti-tumor efficacy was observed, but not to the same degree as in ADA-negative mice dosed with 3 mg/kg mDTA-1. The lack of complete antitumor efficacy may be due to limited intratumoral receptor engagement, compared with receptor engagement in circulation. Overall, this supports a correlation between GITR engagement and antitumor efficacy, and critically, that restoration of antitumor efficacy was possible.

Recently, the development of novel routes of administration, such as intratumoral dosing (Marabelle et al. 2013, 2014), have been evaluated as an option to limit systemic T cell activation while

Pr Proprietary

Downloaded from jpet.aspetjournals.org at ASPET Journals on April 16, 2024

JPET Fast Forward. Published on December 15, 2015 as DOI: 10.1124/jpet.115.229864
This article has not been copyedited and formatted. The final version may differ from this version.

maintaining intratumoral immune activation and antitumor efficacy. Given that the mDTA-1 ADA response can be overcome *in vivo*, localized GITR activation in the tumor may be sufficient to confer antitumor efficacy. Therefore, our results warrant the preclinical exploration of localized treatments with agonistic therapeutics to explore the dynamics of antitumor efficacy versus ADA responses.

Given recent trends of cancer immunotherapy towards employing combinations of various IMR agonists and antagonists (Lu et al. 2014, Blank et al. 2014, Westin et al. 2014), our study sought to characterize whether repeated administration of mDTA-1 an agonist anti-GITR antibody would enhance ADA to a coadministered anti-PD-1 antibody (muDX400). Our results suggest that while mDTA-1 elicits a rapid anti-drug response, it is specific to mDTA-1, and muDX400 pharmacokinetics and disposition are not impacted, at least in the duration of the study. This does not preclude the possibility of an eventual anti-muDX400 response, but we can infer that treatment with mDTA-1 will not necessarily induce a similarly enhanced ADA response to molecules administered simultaneously.

Of importance in our studies is whether the emergence of ADA responses against GITR agonists is translatable to humans. Anaphylaxis induced by anti-drug antibodies against mDTA-1 and OX-86 have already been characterized in preclinical and clinical studies (Murphy et al. 2014, Abramowicz et al. 1992, Baudouin et al. 2003, Werier et al. 1991), Although, the manifestation of immunogenicity in preclinical models are generally not considered predictive to humans, our results suggest that close attention to the appearance of ADA responses should be given when administering T cell agonists. Anti-GITR agonist antibodies are already in the clinic as monotherapy and in combination with anti-PD-1. Ultimately, understanding how the presence of ADAs changes the pharmacokinetics, drug exposure, and clearance of mDTA-1 and muDX400 in mouse models could be helpful for anticipating potential dose adjustments and safety concerns in the clinic, both as monotherapies and in combination.

In conclusion, we showed that exposure to mDTA-1 in mice results in GITR-mediated mDTA-1 immunogenicity leading to the generation of neutralizing anti-drug antibodies, formation of drug-anti-drug immune complexes, rapid mDTA-1 clearance, hepatic disposition, and catabolism. Likewise, we observed diminished target engagement and loss of mDTA-1 antitumor efficacy in mice with pre-existing ADA. Critically, mDTA-1 antitumor efficacy in CT26 and MC38 murine syngeneic tumor models could be

Pr Proprietary

Downloaded from jpet.aspetjournals.org at ASPET Journals on April 16, 2024

JPET Fast Forward. Published on December 15, 2015 as DOI: 10.1124/jpet.115.229864
This article has not been copyedited and formatted. The final version may differ from this version.

partially restored at pharmacological doses that reestablish target engagement on circulating $CD3^+$ $CD4^+$ T cells in ADA positive mice. We also demonstrated that mDTA-1 did not impact the pharmacology of muDX400 when dosed in combination. Taken together, our results facilitate a better understanding of ADA responses against immuno-modulatory monoclonal antibodies and the role of target engagement in regulating drug pharmacology.

Downloaded from jpet.aspetjournals.org at ASPET Journals on April 16, 2024

Proprietary

JPET Fast Forward. Published on December 15, 2015 as DOI: 10.1124/jpet.115.229864
This article has not been copyedited and formatted. The final version may differ from this version.

9. Acknowledgements

We would like to acknowledge the contributions of Drs. Laurence Fayadat-Dilman and Brian Reardon at the Department of Protein Sciences for providing the mDTA-1, muDX400, and VP2 antibodies; Priscilla Lapresca for Animal Facility support; Dr. Wolfgang Seghezzi at the Department of Bioanalytics for MSD and ELISA assay support; Drs. Terri McClanahan, Fernando Ugarte, and Doug Wilson at the Department of Profiling & Expression for support of flow cytometry facilities & equipment, and Drs. Jennifer Yearley, Meric Ovacik, Mohammad Tabrizifard for valuable discussions.

Downloaded from jpet.aspetjournals.org at ASPET Journals on April 16, 2024

Pr Proprietary

JPET Fast Forward. Published on December 15, 2015 as DOI: 10.1124/jpet.115.229864
This article has not been copyedited and formatted. The final version may differ from this version.

10. Authorship Contributions.

Participated in research design: Brunn, Beebe, and Escandon
Conducted experiments: Brunn, Mauze, Gu, Wiswell
Contributed new reagents or analytic tools: Brunn, Mauze, Gu, Zhang, Hodges, Escandon
Performed data analysis: Brunn, Mauze, Gu, Zhang
Wrote or contributed to the writing of the manuscript: Brunn and Escandon.

Downloaded from jpet.aspetjournals.org at ASPET Journals on April 16, 2024

Proprietary

JPET Fast Forward. Published on December 15, 2015 as DOI: 10.1124/jpet.115.229864
This article has not been copyedited and formatted. The final version may differ from this version.

11. References

Abramowicz, D., Crusiaux, A., & Goldman, M. (1992). Anaphylactic shock after retreatment with OKT3 monoclonal antibody. *N Engl J Med* **327**: 736.

Alvarez, H. M., So, O. Y., Hsieh, S., Shinsky-Bjorde, N., Ma, H., Song, Y., & Escandón, E. (2012). Effects of PEGylation and immune complex formation on the pharmacokinetics and biodistribution of recombinant interleukin 10 in mice. *Drug Metabolism and Disposition* **40**: 360-373.

Badylak, S. F., & Gilbert, T. W. (2008, April). Immune response to biologic scaffold materials. In *Seminars in immunology* (Vol. 20, No. 2) pp. 109-116. Academic Press, New York.

Baudouin, V., Crusiaux, A., Haddad, E., Schandene, L., Goldman, M., Loirat, C., & Abramowicz, D. (2003). Anaphylactic shock caused by immunoglobulin E sensitization after retreatment with the chimeric anti–interleukin-2 receptor monoclonal antibody basiliximab. *Transplantation* **76**: 459-463.

Beck, A., Wurch, T., Bailly, C., & Corvaia, N. (2010). Strategies and challenges for the next generation of therapeutic antibodies. *Nature Reviews Immunology* **10**: 345-352.

Blank, C. U. (2014). The perspective of immunotherapy: new molecules and new mechanisms of action in immune modulation. *Current opinion in oncology* **26**: 204-214.

Bogers, W. M. J. M., STAD, R. K., Janssen, D. J., ROOIJEN, N., & DAHA, M. (1991). Kupffer cell depletion in vivo results in preferential elimination of IgG aggregates and immune complexes via specific Fc receptors on rat liver endothelial cells. *Clinical & Experimental Immunology* **86**: 328-333.

Bourdage, J. S., Cook, C. A., Farrington, D. L., Chain, J. S., & Konrad, R. J. (2007). An Affinity Capture Elution (ACE) assay for detection of anti-drug antibody to monoclonal antibody therapeutics in the presence of high levels of drug. *Journal of immunological methods* **327**: 10-17.

Pr Proprietary

Downloaded from jpet.aspetjournals.org at ASPET Journals on April 16, 2024

JPET Fast Forward. Published on December 15, 2015 as DOI: 10.1124/jpet.115.229864
This article has not been copyedited and formatted. The final version may differ from this version.

Brennan, F. R., Morton, L. D., Spindeldreher, S., Kiessling, A., Allenspach, R., Hey, A., & Sims, J. (2010). Safety and immunotoxicity assessment of immunomodulatory monoclonal antibodies. In *MAbs* (Vol. 2, No. 3) pp. 233-255. Taylor & Francis, New York.

Chirino, A. J., Ary, M. L., & Marshall, S. A. (2004). Minimizing the immunogenicity of protein therapeutics. *Drug discovery today*, **9**: 82-90.

Clarke, J. B. (2010). Mechanisms of adverse drug reactions to biologics. In *Adverse Drug Reactions* pp. 453-474, Springer Publishers, Germany.

Coe, D., Begom, S., Addey, C., White, M., Dyson, J., & Chai, J. G. (2010). Depletion of regulatory T cells by anti-GITR mAb as a novel mechanism for cancer immunotherapy. *Cancer Immunology, Immunotherapy* **59**: 1367-1377.

Cohen, A. D., Diab, A., Perales, M. A., Wolchok, J. D., Rizzuto, G., Merghoub, T., & Houghton, A. N. (2006). Agonist anti-GITR antibody enhances vaccine-induced CD8+ T-cell responses and tumor immunity. *Cancer research* **66**: 4904-4912.

Cohen, A. D., Schaer, D. A., Liu, C., Li, Y., Hirschhorn-Cymmerman, D., Kim, S. C., & Wolchok, J. D. (2010). Agonist anti-GITR monoclonal antibody induces melanoma tumor immunity in mice by altering regulatory T cell stability and intra-tumor accumulation. *PLoS One* **5**: e10436.

Croft, M., Benedict, C. A., & Ware, C. F. (2013). Clinical targeting of the TNF and TNFR superfamilies. *Nature Reviews Drug Discovery* **12**: 147-168.

De Groot, A. S., & Martin, W. (2009). Reducing risk, improving outcomes: bioengineering less immunogenic protein therapeutics. *Clinical Immunology* **131**: 189-201.

Pr Proprietary

Downloaded from jpet.aspetjournals.org at ASPET Journals on April 16, 2024

JPET Fast Forward. Published on December 15, 2015 as DOI: 10.1124/jpet.115.229864
This article has not been copyedited and formatted. The final version may differ from this version.

De Groot, A. S., & Moise, L. (2007). Prediction of immunogenicity for therapeutic proteins: state of the art. *Current Opinion in Drug Discovery and Development* **10**: 332.

Ganesan, L. P., Kim, J., Wu, Y., Mohanty, S., Phillips, G. S., Birmingham, D. J.,& Anderson, C. L. (2012). FcγRIIb on liver sinusoidal endothelium clears small immune complexes. *The Journal of Immunology* **189**: 4981-4988.

Hamid, O., Robert, C., Daud, A., Hodi, F. S., Hwu, W. J., Kefford, R., & Ribas, A. (2013). Safety and tumor responses with lambrolizumab (anti–PD-1) in melanoma. *New England Journal of Medicine* **369**: 134-144.

Hansel, T. T., Kropshofer, H., Singer, T., Mitchell, J. A., & George, A. J. (2010). The safety and side effects of monoclonal antibodies. *Nature reviews Drug discovery* **9**: 325-338.

Hirsch, H. A., Pinheiro, E. M., Cai, M., Ma, Y., Sathe, M., Ayers, M., & McClanahan, T. K. (2015). Molecular characterization of mouse syngeneic tumor models in response to treatment with anti-PD-1 immunotherapy. *Cancer Research* **75**: 1328-1328.

Hodi, F. S., O'Day, S. J., McDermott, D. F., Weber, R. W., Sosman, J. A., Haanen, J. B., & Urba, W. J. (2010). Improved survival with ipilimumab in patients with metastatic melanoma. *New England Journal of Medicine* **363**: 711-723.

Kanamaru, F., Youngnak, P., Hashiguchi, M., Nishioka, T., Takahashi, T., Sakaguchi, S., & Azuma, M. (2004). Costimulation via glucocorticoid-induced TNF receptor in both conventional and CD25+ regulatory CD4+ T cells.*The Journal of Immunology* **172**: 7306-7314.

Downloaded from jpet.aspetjournals.org at ASPET Journals on April 16, 2024

Pr Proprietary

JPET Fast Forward. Published on December 15, 2015 as DOI: 10.1124/jpet.115.229864
This article has not been copyedited and formatted. The final version may differ from this version.

Kelley, M., Ahene, A. B., Gorovits, B., Kamerud, J., King, L. E., McIntosh, T., & Yang, J. (2013). Theoretical considerations and practical approaches to address the effect of anti-drug antibody (ADA) on quantification of biotherapeutics in circulation. *The AAPS journal* **15**: 646-658.

Kohm, A. P., Williams, J. S., & Miller, S. D. (2004). Cutting edge: ligation of the glucocorticoid-induced TNF receptor enhances autoreactive CD4+ T cell activation and experimental autoimmune encephalomyelitis. *The Journal of Immunology* **172**: 4686-4690.

Kurlander, R. J., Ellison, D. M., & Hall, J. (1984). The blockade of Fc receptor-mediated clearance of immune complexes in vivo by a monoclonal antibody (2.4 G2) directed against Fc receptors on murine leukocytes. *The Journal of Immunology* **133**: 855-862.

Li, P. Z., Li, J. Z., Li, M., Gong, J. P., & He, K. (2014). An efficient method to isolate and culture mouse Kupffer cells. *Immunology letters* **158**: 52-56.

Lovdal, T., Andersen, E., Brech, A., & Berg, T. (2000). Fc receptor mediated endocytosis of small soluble immunoglobulin G immune complexes in Kupffer and endothelial cells from rat liver. *Journal of cell science* **113**: 3255-3266.

Lu, L., Xu, X., Zhang, B., Zhang, R., Ji, H., & Wang, X. (2014). Combined PD-1 blockade and GITR triggering induce a potent antitumor immunity in murine cancer models and synergizes with chemotherapeutic drugs. *J Transl Med* **12**: 36.

Marabelle, A., Kohrt, H., Caux, C., & Levy, R. (2014). Intratumoral immunization: a new paradigm for cancer therapy. *Clinical Cancer Research* **20**: 1747-1756.

Downloaded from jpet.aspetjournals.org at ASPET Journals on April 16, 2024

Pr Proprietary

JPET Fast Forward. Published on December 15, 2015 as DOI: 10.1124/jpet.115.229864
This article has not been copyedited and formatted. The final version may differ from this version.

Marabelle, A., Kohrt, H., Sagiv-Barfi, I., Ajami, B., Axtell, R. C., Zhou, G.,& Levy, R. (2013). Depleting tumor-specific Tregs at a single site eradicates disseminated tumors. *The Journal of clinical investigation* **123**: 2447.

Melero, I., Hervas-Stubbs, S., Glennie, M., Pardoll, D. M., & Chen, L. (2007). Immunostimulatory monoclonal antibodies for cancer therapy. *Nature Reviews Cancer* **7**: 95-106.

Murata, S., Ladle, B. H., Kim, P. S., Lutz, E. R., Wolpoe, M. E., Ivie, S. E., & Reilly, R. T. (2006). OX40 costimulation synergizes with GM-CSF whole-cell vaccination to overcome established CD8+ T cell tolerance to an endogenous tumor antigen. *The Journal of Immunology* **176**: 974-983.

Murphy, J. T., Burey, A. P., Beebe, A. M., Gu, D., Presta, L. G., Merghoub, T., & Wolchok, J. D. (2014). Anaphylaxis caused by repetitive doses of a GITR agonist monoclonal antibody in mice. *Blood* **123**: 2172-2180.

Nishikawa, H., Kato, T., Hirayama, M., Orito, Y., Sato, E., Harada, N., & Shiku, H. (2008). Regulatory T Cell–Resistant CD8+ T Cells Induced by Glucocorticoid-Induced Tumor Necrosis Factor Receptor Signaling. *Cancer Research* **68**: 5948-5954.

Nlend, M. C., Desai, S., Hong, S. J., Anderson, M. B., Los, G. V., Hermanson, G. T., & Bell, P. A. (2014). Biodistribution and clearance of non-targeted DyLight dyes in tumor-free nude mice for in vivo imaging. *Cancer Research* **74**: 4305-4305.

Nocentini, G., & Riccardi, C. (2005). GITR: a multifaceted regulator of immunity belonging to the tumor necrosis factor receptor superfamily. *European journal of immunology* **35**: 1016-1022.

Page, D. B., Postow, M. A., Callahan, M. K., Allison, J. P., & Wolchok, J. D. (2014). Immune modulation in cancer with antibodies. *Annual review of medicine* **65**: 185-202.

Downloaded from jpet.aspetjournals.org at ASPET Journals on April 16, 2024

Pr Proprietary

JPET Fast Forward. Published on December 15, 2015 as DOI: 10.1124/jpet.115.229864
This article has not been copyedited and formatted. The final version may differ from this version.

Peggs, K. S., Quezada, S. A., & Allison, J. P. (2009). Cancer immunotherapy: co-stimulatory agonists and co-inhibitory antagonists. *Clinical & Experimental Immunology* **157**: 9-19.

Pepinsky, R. B., LePage, D. J., Gill, A., Chakraborty, A., Vaidyanathan, S., Green, M., & Martin, P. (2001). Improved pharmacokinetic properties of a polyethylene glycol-modified form of interferon-β-1a with preserved in vitro bioactivity. *Journal of Pharmacology and Experimental Therapeutics* **297***:* 1059-1066.

Pinheiro, E. M., Mangadu, R., Phan, U. T., Cai, M., Ma, Y., Hirsch, H. A., ... & Long, B. J. (2015). Evaluation of the antitumor activity of anti-PD-1 immunotherapy as a single agent and in combination with approved agents in preclinical tumor models. *Cancer Research* **75:** 269-269.

Reichert, J. M. (2011). Antibody-based therapeutics to watch in 2011. In *MAbs* (Vol. 3, No. 1) pp. 76-99 Taylor & Francis, New York.

Reuben, J. M., Lee, B. N., Li, C., Gomez-Navarro, J., Bozon, V. A., Parker, C. A., & Camacho, L. H. (2006). Biologic and immunomodulatory events after CTLA-4 blockade with ticilimumab in patients with advanced malignant melanoma. *Cancer* **106**: 2437-2444.

Robert, C., Thomas, L., Bondarenko, I., O'Day, S., Weber, J., Garbe, C., & Wolchok, J. D. (2011). Ipilimumab plus dacarbazine for previously untreated metastatic melanoma. *New England Journal of Medicine* **364**: 2517-2526.

Rojas, J. R., Taylor, R. P., Cunningham, M. R., Rutkoski, T. J., Vennarini, J., Jang, H., & Wagner, C. L. (2005). Formation, distribution, and elimination of infliximab and anti-infliximab immune complexes in cynomolgus monkeys.*Journal of Pharmacology and Experimental Therapeutics* **313**: 578-585.

Downloaded from jpet.aspetjournals.org at ASPET Journals on April 16, 2024

Pr Proprietary

JPET Fast Forward. Published on December 15, 2015 as DOI: 10.1124/jpet.115.229864
This article has not been copyedited and formatted. The final version may differ from this version.

Ronchetti, S., Zollo, O., Bruscoli, S., Agostini, M., Bianchini, R., Nocentini, G., & Riccardi, C. (2004). Frontline: GITR, a member of the TNF receptor superfamily, is costimulatory to mouse T lymphocyte subpopulations.*European journal of immunology* **34**: 613-622.

Schaer, D. A., Murphy, J. T., & Wolchok, J. D. (2012). Modulation of GITR for cancer immunotherapy. *Current opinion in immunology* **24**: 217-224.

Shankar, G., Shores, E., Wagner, C., & Mire-Sluis, A. (2006). Scientific and regulatory considerations on the immunogenicity of biologics. *Trends in biotechnology* **24**: 274-280.

Shankar, G., Pendley, C., & Stein, K. E. (2007). A risk-based bioanalytical strategy for the assessment of antibody immune responses against biological drugs. *Nature biotechnology* **25**: 555-561.

Sugamura, K., Ishii, N., & Weinberg, A. D. (2004). Therapeutic targeting of the effector T-cell co-stimulatory molecule OX40. *Nature Reviews Immunology* **4**: 420-431.

Suntharalingam, G., Perry, M. R., Ward, S., Brett, S. J., Castello-Cortes, A., Brunner, M. D., & Panoskaltsis, N. (2006). Cytokine storm in a phase 1 trial of the anti-CD28 monoclonal antibody TGN1412. *New England Journal of Medicine* **355**: 1018-1028.

Tone, M., Tone, Y., Adams, E., Yates, S. F., Frewin, M. R., Cobbold, S. P., & Waldmann, H. (2003). Mouse glucocorticoid-induced tumor necrosis factor receptor ligand is costimulatory for T cells. *Proceedings of the National Academy of Sciences* **100:** 15059-15064.

Topalian, S. L., Hodi, F. S., Brahmer, J. R., Gettinger, S. N., Smith, D. C., McDermott, D. F., & Sznol, M. (2012). Safety, activity, and immune correlates of anti–PD-1 antibody in cancer. *New England Journal of Medicine* **366**: 2443-2454.

Downloaded from jpet.aspetjournals.org at ASPET Journals on April 16, 2024

Pr Proprietary

JPET Fast Forward. Published on December 15, 2015 as DOI: 10.1124/jpet.115.229864
This article has not been copyedited and formatted. The final version may differ from this version.

Werier, J., Cheung, A. S., & Matas, A. (1991). Anaphylactic hypersensitivity reaction after repeat OKT3 treatment. *The Lancet* **337**: 1351.

Westin, J. R., Chu, F., Zhang, M., Fayad, L. E., Kwak, L. W., Fowler, N., ... & Neelapu, S. S. (2014). Safety and activity of PD1 blockade by pidilizumab in combination with rituximab in patients with relapsed follicular lymphoma: a single group, open-label, phase 2 trial. *The Lancet Oncology* **15**: 69-77.

Wolchok, J. D., Kluger, H., Callahan, M. K., Postow, M. A., Rizvi, N. A., Lesokhin, A. M., & Sznol, M. (2013). Nivolumab plus ipilimumab in advanced melanoma. *New England Journal of Medicine*, **369**:122-133.

Zeng, W. Q., Zhang, J. Q., Li, Y., Yang, K., Chen, Y. P., & Liu, Z. J. (2013). A new method to isolate and culture rat kupffer cells. *PLoS ONE* **8:** 8

Zhou, P., L'italien, L., Hodges, D., & Schebye, X. M. (2007). Pivotal roles of CD4+ effector T cells in mediating agonistic anti-GITR mAb-induced-immune activation and tumor immunity in CT26 tumors. *The Journal of Immunology* **179**: 7365-7375.

Zhou, P., Qiu, J., L'Italien, L., Gu, D., Hodges, D., Chao, C. C., & Schebye, X. M. (2010). Mature B cells are critical to T-cell-mediated tumor immunity induced by an agonist anti-GITR monoclonal antibody. *Journal of Immunotherapy* **33**: 789-797.

Downloaded from jpet.aspetjournals.org at ASPET Journals on April 16, 2024

Pr Proprietary

JPET Fast Forward. Published on December 15, 2015 as DOI: 10.1124/jpet.115.229864
This article has not been copyedited and formatted. The final version may differ from this version.

12. Footnotes

a) This work was supported by Merck Research Laboratories (MRL), Merck & Co. Inc. The MRL Postdoctoral Research Program provided financial support of NDB.

Downloaded from jpet.aspetjournals.org at ASPET Journals on April 16, 2024

Proprietary

JPET Fast Forward. Published on December 15, 2015 as DOI: 10.1124/jpet.115.229864
This article has not been copyedited and formatted. The final version may differ from this version.

13. Figure Legends

Figure 1. The concentration time profiles of mDTA-1 in naïve BALB/c mice (A) and littermates previously dosed 3 mg/kg mDTA-1 q7d x 2 (B). Both cohorts were injected subcutaneously with 5, or 30 mg/kg of DyLight-labeled mDTA-1 and the concentrations were determined by fluorescence linked emission assays. Data are representative of 2 independent experiments (n = 3 mice per group). Error bars correspond to S.D. calculated using GraphPad Prism 6.

Figure 2. Plasma samples from naïve (A) and mDTA-1 pretreated (B) BALB/c mice subcutaneously dosed with 30 mg/kg DyLight labeled mDTA-1. Specimens were collected at 4, 8, 16, 24, 48, and 96 hour time points and characterized by SEC HPLC analysis as described in *Materials and Methods*. The retention time of 8.1 minutes corresponds with a theoretical molecular weight of ~155,000 kDa on the Phenomenex 3000 indicating the major peaks corresponds to intact monomeric mDTA-1 monoclonal antibody. The scale of the x-axis has been expanded to highlight the high molecular weight complexes present in (B) indicated by an (*). Data are representative of 2 independent experiments (n = 3 mice per group).

Figure 3. High molecular weight complex formation in plasma samples from mDTA-1 pretreated mice spiked *in vitro* with the indicated concentrations of DyLight 650-mDTA-1. Naïve plasma and an IgG2a isotype antibody were utilized as controls. Aliquots were incubated for 15 minutes at 37ºC prior to SEC-HPLC analysis. The retention time of 8.1 minutes corresponds with a theoretical molecular weight of ~155,000 kDa. The high molecular weight complexes are indicated by an (*). Data are representative of 2 independent experiments (n = 3 mice per group).

Figure 4. Tissue distribution of DyLight-650 labeled mDTA-1 in naïve (A, B), and mDTA-1 pretreated (C,D) BALB/c mice subcutaneously dosed with 30 mg/kg mDTA-1. Drug concentrations were determined by FELA as described in material and methods. Tissue/blood ratios greater than 1 are indicative of tissue uptake (A, C) and mDTA-1 concentration (microgram/mL) was measured at 4, 8, 16, 24, 48, and 96 hours

Downloaded from jpet.aspetjournals.org at ASPET Journals on April 16, 2024

Pr Proprietary

JPET Fast Forward. Published on December 15, 2015 as DOI: 10.1124/jpet.115.229864
This article has not been copyedited and formatted. The final version may differ from this version.

after dosing (B, D). Data are representative of 2 independent experiments (n = 3 mice per group) and error bars correspond to S.D. calculated using GraphPad Prism 6.

Figure 5. Plasma and liver lysates of naïve (A) and pretreated (B) BALB/c mice subcutaneously dosed with 30 mg/kg labeled mDTA-1 were collected at 4, 8, 16, 24, 48, and 96 hours and characterized by CAFÉ. Arrows indicate the presence of antibody derived catabolites.

Figure 6. Fluorescent microscopy of Kupffer cells (KCs) from naïve and mDTA-1 pretreated BALB/c mice subcutaneously dosed with 30 mg/kg DyLight-650 labeled mDTA-1. KCs were isolated by gradient centrifugation as described in the *Materials and Methods.* DyLight 488 labeled anti-F4/F80 monoclonal antibody (green) was used for KC identification. The fluorescent and transmitted light signals were overlaid using the EVOS FL Cell Imaging System (Life Technologies). White bar corresponds to 50 µM. All images were representative of typical cell fluorescence and morphology. The experiment was replicated three times with identical results.

Figure 7. Wild type and GITR-/- BALB/c mice pretreated with mDTA-1 were given a SC dose of 3mg/kg unlabeled mDTA-1. Plasma samples were taken at 3, 30, 60, 90, and 120 days and examined for anti-drug antibodies using a Meso Scale Discovery bridging immunogenicity assay (A), and for mDTA-1 concentrations by direct ELISA (B). Experiments were carried out in duplicate, n=6 mice per time point, and error bars correspond to ±S.D. calculated using GraphPad Prism 6.

Figure 8. Dose escalation of mDTA-1 in ADA positive mice restores antitumor efficacy. C57BL/6J and BALB/cAnN mice split into groups that were either subcutaneously pretreated with mDTA-1 to establish an ADA (+) response, or were not pretreated and remained ADA (-). The BALB/c mice were implanted with CT-26 tumors (A, B) and C57BL/6 mice were implanted with MC38 tumors (C,D). Upon reaching an average of approximately 100mm^3, mice were treated with mDTA-1 as a single dose on day 0, or in multiple doses on days 0, 7, and 14 at the indicated dosages. Mean tumor volume (mm^3) ± SEM, n=10 mice per condition, was plotted with respect to time (A, C) and the individual tumor volumes were

Downloaded from jpet.aspetjournals.org at ASPET Journals on April 16, 2024

Pr Proprietary

JPET Fast Forward. Published on December 15, 2015 as DOI: 10.1124/jpet.115.229864
This article has not been copyedited and formatted. The final version may differ from this version.

compared at day 21 for CT26 (B) or day 18 MC38 (D). Median tumor volume for respective cohort plotted as horizontal bar, and *P<0.05 and ****P<0.0001 compared to isotype control based on Mann-Whitney *U*-test calculated in GraphPad Prism 6 (B, D)

Figure 9. ADAs impair mDTA-1 engagement of GITR on $CD3^+$ $CD4^+$ T cells. Naïve and pretreated mDTA-1 BALB/c mice were injected SC with 3 or 30 mg/kg of unlabeled mDTA-1, DyLight 650-mDTA-1 or DyLight 650 labeled IgG2a isotype control antibody. Peripheral blood mononuclear cells (PBMCs) were isolated from whole blood 4 hours later as previously described in *Materials and Methods.* Fluorescence activated cell sorting (FACS) was used to select $CD3^+$ $CD4^+$ T cells from PBMCs and quantify the percent of GITR engagement (A). The mean fluorescent intensity (MFI) of cells incubated ex-vivo in the absence of antibody or incubated with 5µg/mL DyLight 650-mDTA-1 were used as negative and positive GITR binding controls respectively (A). $CD3^+$ $CD4^+$ T cells isolated from naïve vs. ADA positive mice dosed with fluorescent mDTA-1 (3 and 30 mg/kg respectively) were also imaged on an EVOS FL fluorescent microscope (B). Images were representative of prevailing cell fluorescence and morphology. Typical FACS-MFI shifts for $CD3^+$ $CD4^+$ T cells in all study groups were plotted using FlowJo (C). All *in vivo* target engagement and FACS Experiments were carried out in duplicate, n=3 mice per time point, and error bars correspond to ±S.D. calculated using GraphPad Prism 6 and error bars correspond to S.D. calculated using GraphPad Prism 6.

Figure 10. Concentration time profiles of PD-1 antagonist muDX400 in naïve, muX400, and muX400 + mDTA-1 pretreated BALB/c mice. Cohorts were dosed subcutaneously with 30 mg/kg of DyLight 650 labeled muDX400 (A, B, C) or mDTA-1 (D) and the concentrations were determined by FELA as previously described. N=3 mice per group and error bars correspond to S.D. calculated using GraphPad Prism 6.

Figure 11. Tissue distribution of DyLight-650 labeled muDX400 (30mg/kg SC) in BALB/c mice pretreated with muDX400 alone (A, B) or muDX400 + mDTA-1 (C, D). Drug concentrations were determined by FELA. Tissue/blood ratios greater than 1 are indicative of tissue uptake (A) (C). MuDX400 concentrations

Pr Proprietary

Downloaded from jpet.aspetjournals.org at ASPET Journals on April 16, 2024

JPET Fast Forward. Published on December 15, 2015 as DOI: 10.1124/jpet.115.229864
This article has not been copyedited and formatted. The final version may differ from this version.

(microgram/mL) were measured at 4, 8, 16, 24, 48, and 96 hours (B) (D). N=3 mice per time point and error bars correspond to S.D. calculated using GraphPad Prism 6.

Downloaded from jpet.aspetjournals.org at ASPET Journals on April 16, 2024

Proprietary

JPET Fast Forward. Published on December 15, 2015 as DOI: 10.1124/jpet.115.229864
This article has not been copyedited and formatted. The final version may differ from this version.

14. Tables

Table 1: Pharmacokinetic parameters determined by noncompartmental analysis (WinNonlin).

Pretreatment Regimen	**Dose**	**$t_{1/2}$**	**C_{max}**	**AUC_{last}**	**Cl**	**V_{ss}**
mDTA-1	(mg/kg)	day	µg/mL	(hr*µg/mL)	(mL/day/kg)	(mL/kg)
None	5	3.7	51.1	3536.7	16.7	87.9
None	30	4.0	277.8	18510.8	17.7	101.1
3 mg/kg mDTA-1 q7dx2	5	0.4	2.7	147.0	786.7	906.8
3 mg/kg mDTA-1 q7dx2	30	0.8	75.5	2614.3	273.8	188.1

Downloaded from jpet.aspetjournals.org at ASPET Journals on April 16, 2024

Proprietary

JPET Fast Forward. Published on December 15, 2015 as DOI: 10.1124/jpet.115.229864
This article has not been copyedited and formatted. The final version may differ from this version.

Table 2. Effect of mDTA-1, muDX400 or combination pretreatments in the pharmacokinetics of 650-labeled muDX400 and mDTA-1

Pretreatment Regimen	**DyLight 650 Antibody**	**Dose**	**$t_{1/2}$**	**C_{max}**	**AUC_{last}**	**Cl**	**V_{ss}**
		(mpk)	day	µg/mL	(hr*µg/mL)	(mL/day/kg)	(mL/kg)
mDTA-1 + muDX400 3mg/kg q7dx2	mDTA-1	30	0.5	81.4	3020.6	235.2	178.1
Naïve	muDX400	30	7.3	267.2	20717.6	10.1	106.4
muDX400 3mg/kg q7dx2	muDX400	30	7.4	290.5	22735.5	9.1	97.8
mDTA-1 + muDX400 3mg/kg q7dx2	muDX400	30	8.4	281.6	23259.4	8.2	99.3

Downloaded from jpet.aspetjournals.org at ASPET Journals on April 16, 2024

Pr Proprietary

Figure 1

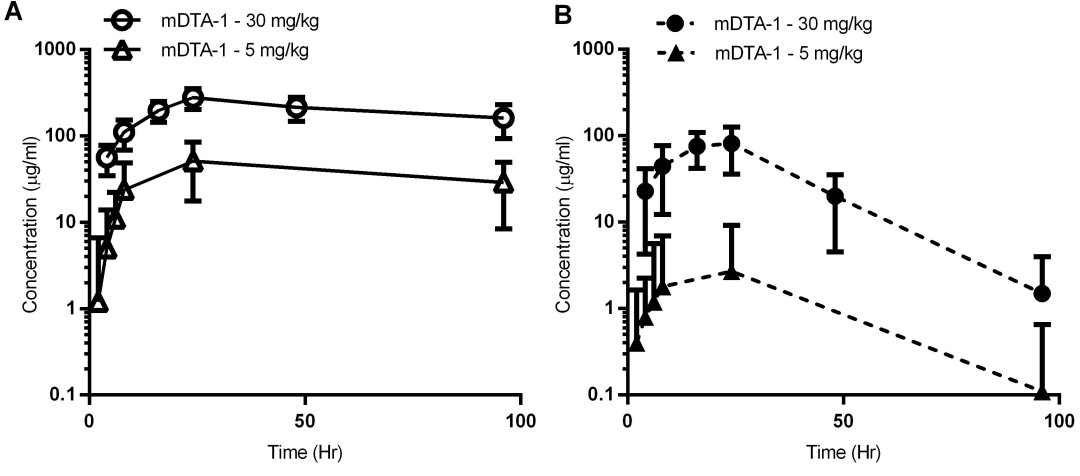
A
mDTA-1 - 30 mg/kg
mDTA-1 - 5 mg/kg
1000
100
10
1
0.1
Concentration (µg/ml)
0
50
100
Time (Hr)
B
mDTA-1 - 30 mg/kg
mDTA-1 - 5 mg/kg
1000
100
10
1
0.1
Concentration (µg/ml)
0
50
100
Time (Hr)

Figure 2

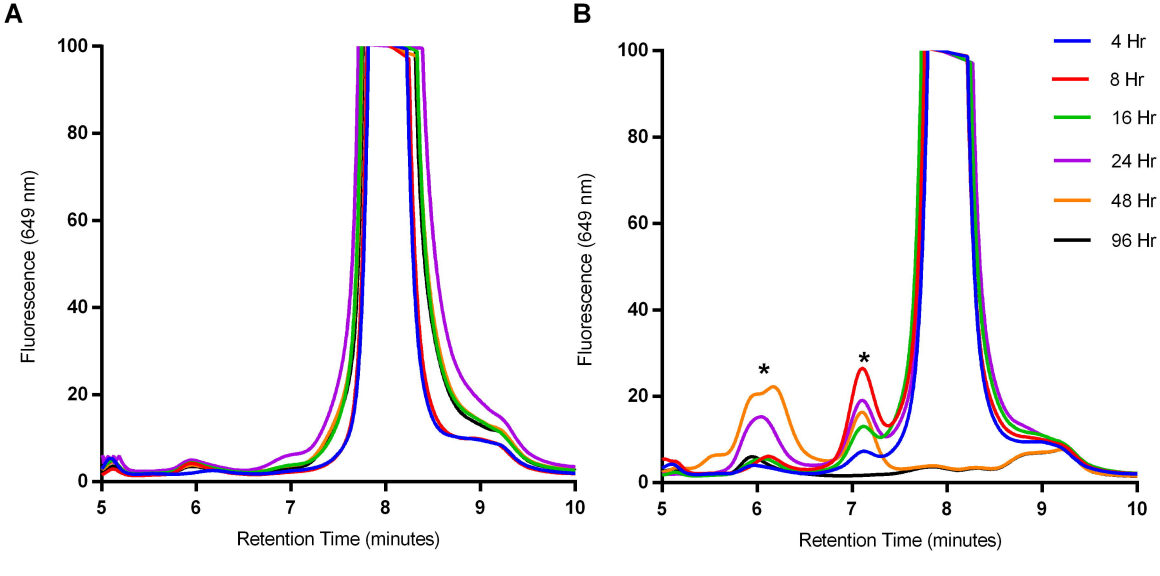
A
B
Fluorescence (649 nm)
Retention Time (minutes)
100
80
60
40
20
0
5
6
7
8
9
10
4 Hr
8 Hr
16 Hr
24 Hr
48 Hr
96 Hr
*
*

Figure 3

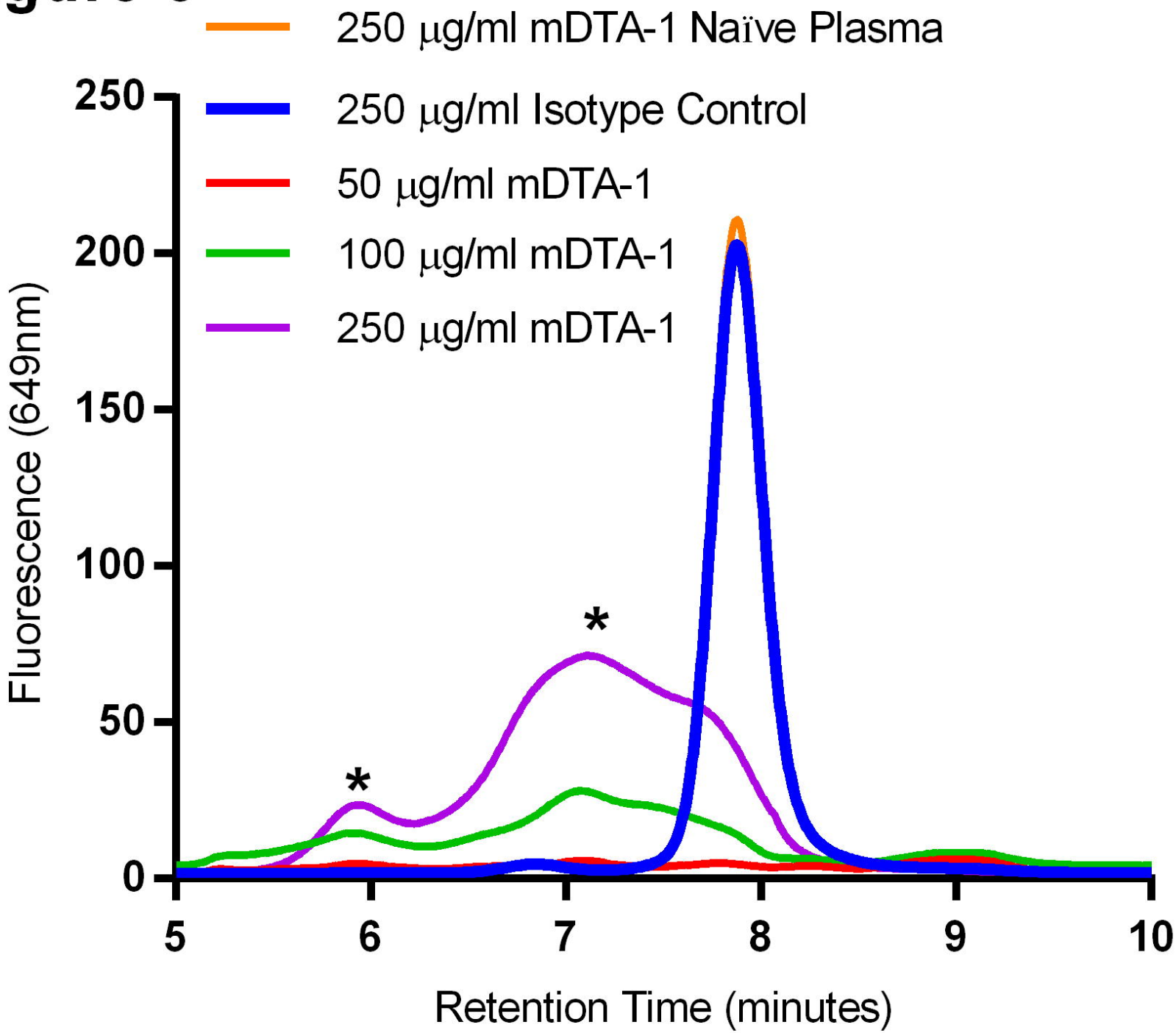
250 μg/ml mDTA-1 Naïve Plasma
250 μg/ml Isotype Control
50 μg/ml mDTA-1
100 μg/ml mDTA-1
250 μg/ml mDTA-1
Fluorescence (649nm)
250
200
150
100
50
0
*
*
5
6
7
8
9
10
Retention Time (minutes)

Figure 4

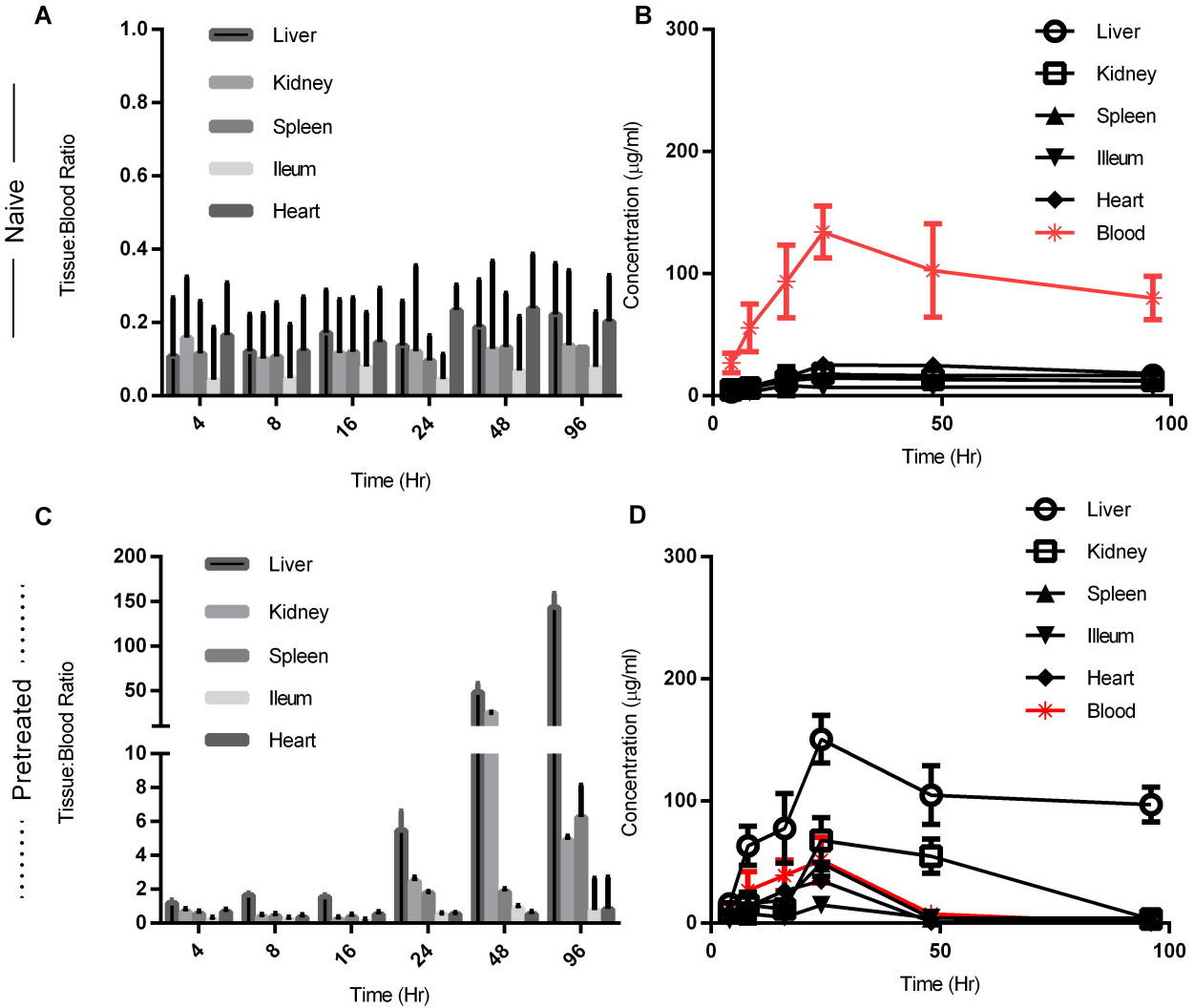
A
B
C
D
Naive
Pretreated
Tissue:Blood Ratio
Concentration (µg/ml)
Time (Hr)
Liver
Kidney
Spleen
Ileum
Heart
Blood
4
8
16
24
48
96
0
50
100
200
300

Figure 5

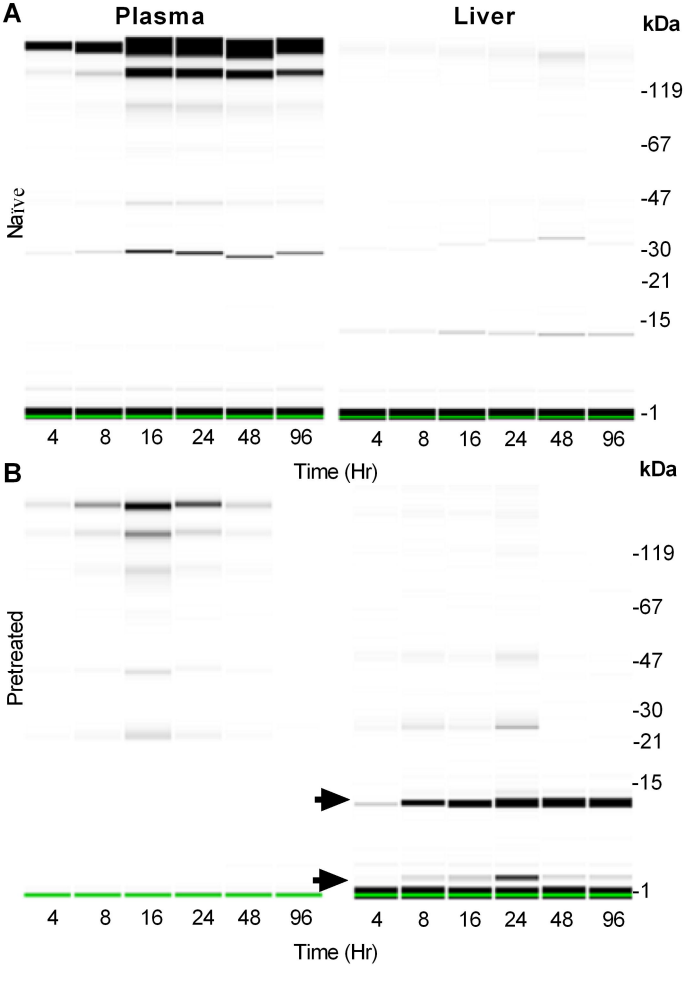
A
Plasma
Liver
kDa
-119
-67
-47
-30
-21
-15
-1
Naïve
4 8 16 24 48 96
4 8 16 24 48 96
Time (Hr)
B
kDa
-119
-67
-47
-30
-21
-15
-1
Pretreated
4 8 16 24 48 96
4 8 16 24 48 96
Time (Hr)

Figure 6

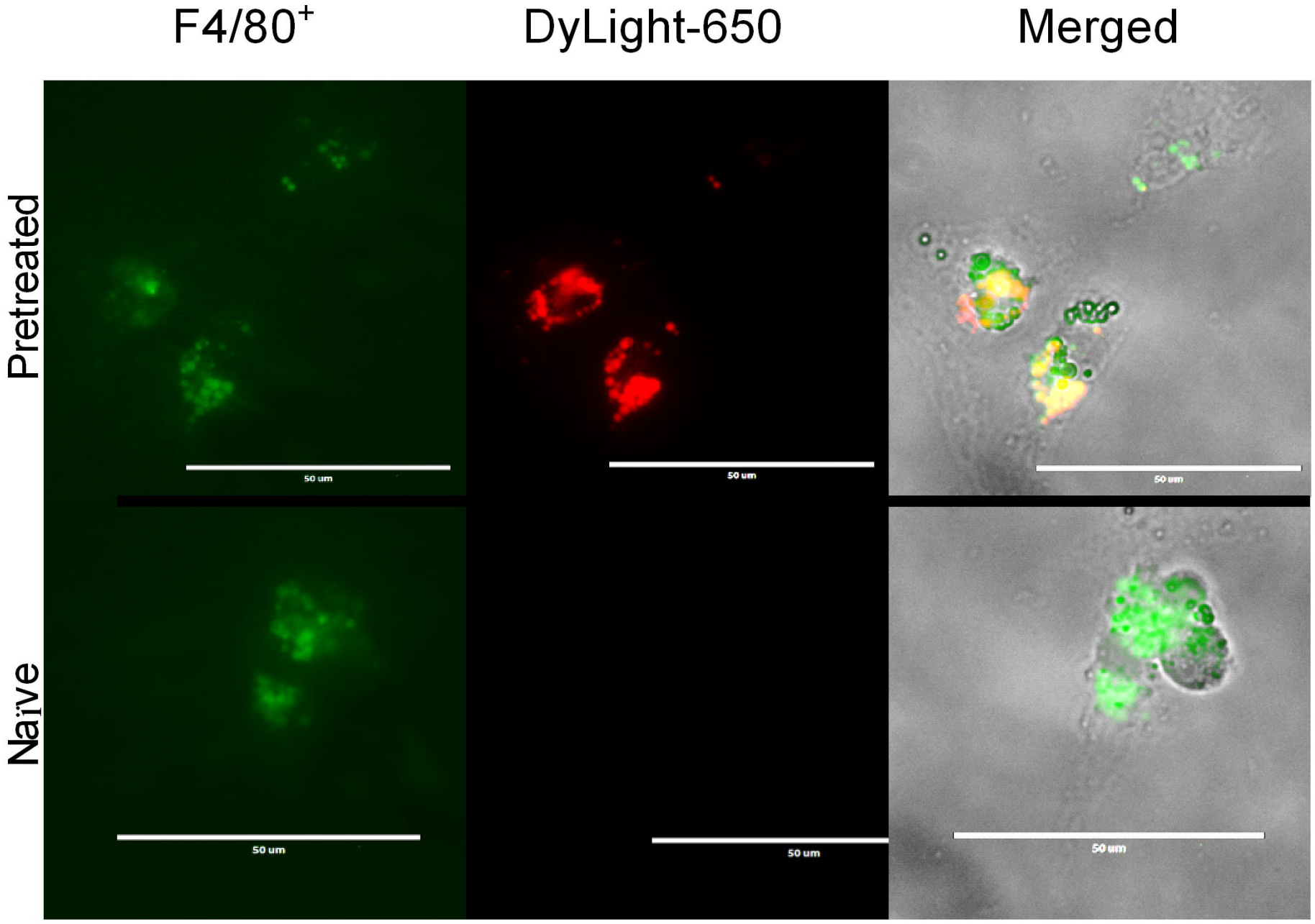
F4/80+
DyLight-650
Merged
Pretreated
Naïve
50 um
50 um
50 um
50 um
50 um

Figure 7

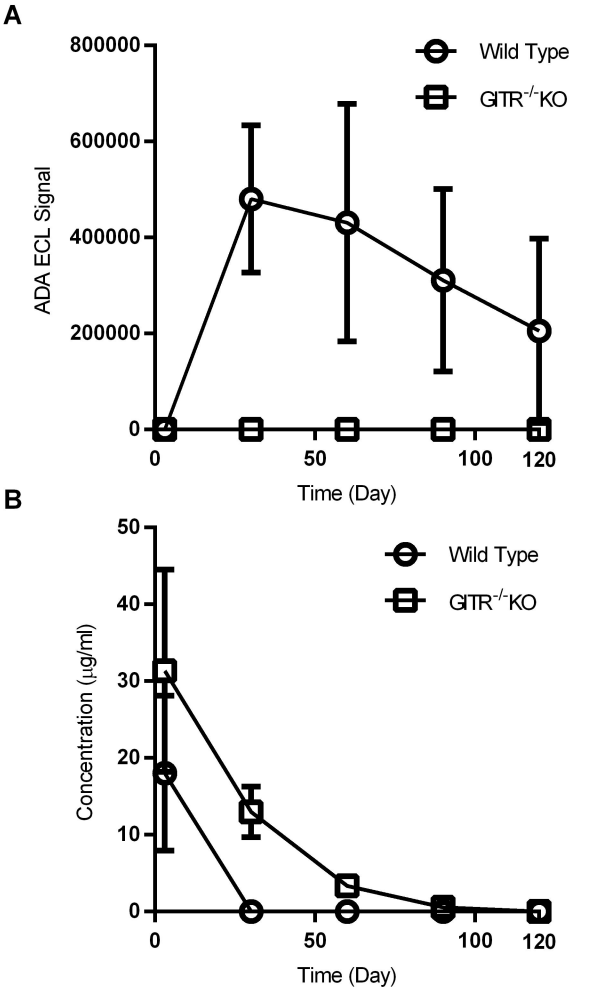
A
800000
600000
400000
200000
0
ADA ECL Signal
Wild Type
GITR-/-KO
0
50
100
120
Time (Day)
B
50
40
30
20
10
0
Concentration (μg/ml)
Wild Type
GITR-/-KO
0
50
100
120
Time (Day)

Figure 8

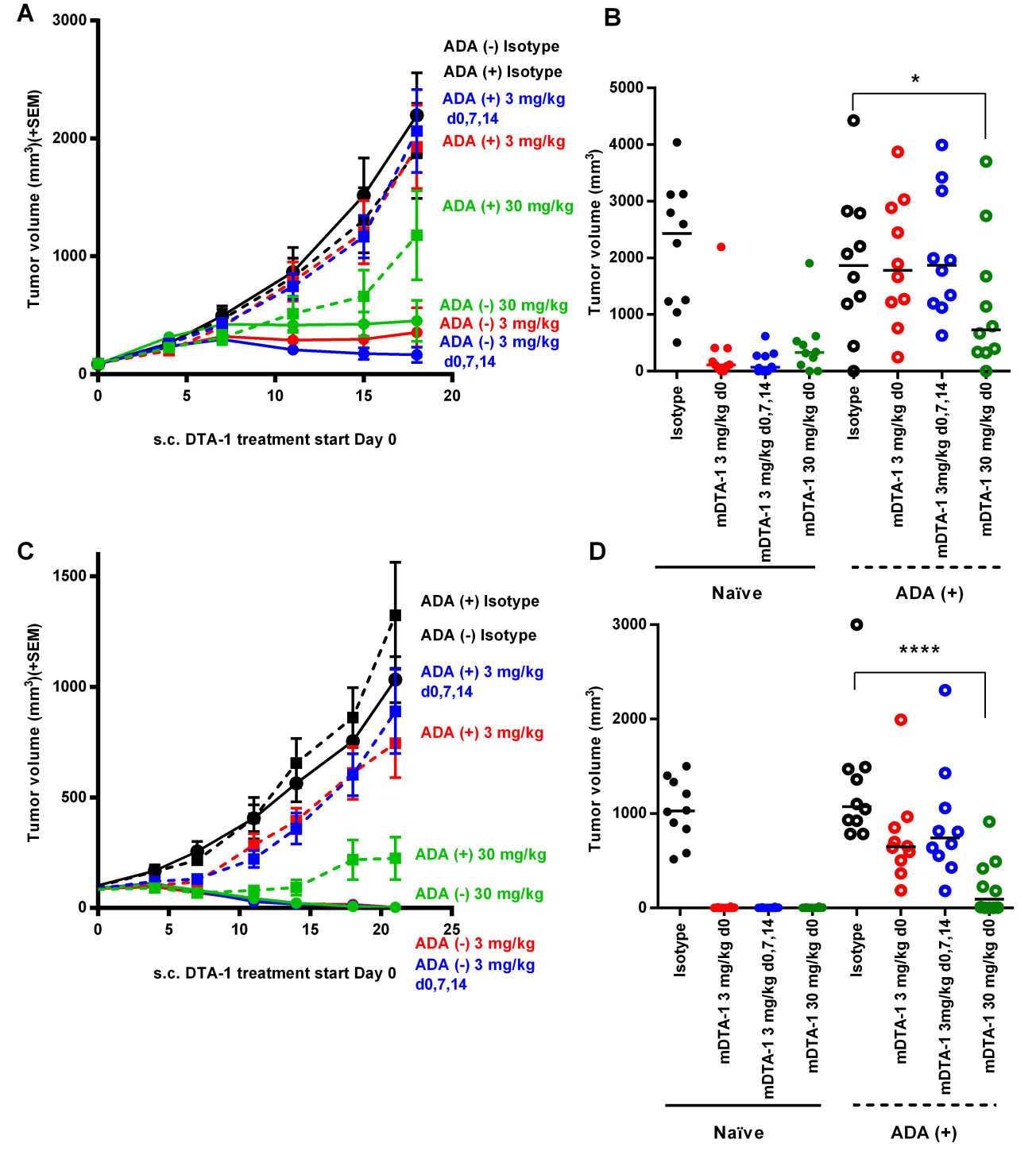
A
Tumor volume (mm3)(+SEM)
s.c. DTA-1 treatment start Day 0
ADA (-) Isotype
ADA (+) Isotype
ADA (+) 3 mg/kg d0,7,14
ADA (+) 3 mg/kg
ADA (+) 30 mg/kg
ADA (-) 30 mg/kg
ADA (-) 3 mg/kg
ADA (-) 3 mg/kg d0,7,14
B
Tumor volume (mm3)
Isotype
mDTA-1 3 mg/kg d0
mDTA-1 3 mg/kg d0,7,14
mDTA-1 30 mg/kg d0
mDTA-1 3mg/kg d0,7,14
Naïve
ADA (+)
C
Tumor volume (mm3)(+SEM)
s.c. DTA-1 treatment start Day 0
ADA (+) Isotype
ADA (-) Isotype
ADA (+) 3 mg/kg d0,7,14
ADA (+) 3 mg/kg
ADA (+) 30 mg/kg
ADA (-) 30 mg/kg
ADA (-) 3 mg/kg
ADA (-) 3 mg/kg d0,7,14
D
Tumor volume (mm3)
Isotype
mDTA-1 3 mg/kg d0
mDTA-1 3 mg/kg d0,7,14
mDTA-1 30 mg/kg d0
mDTA-1 3mg/kg d0,7,14
Naïve
ADA (+)

Figure 9

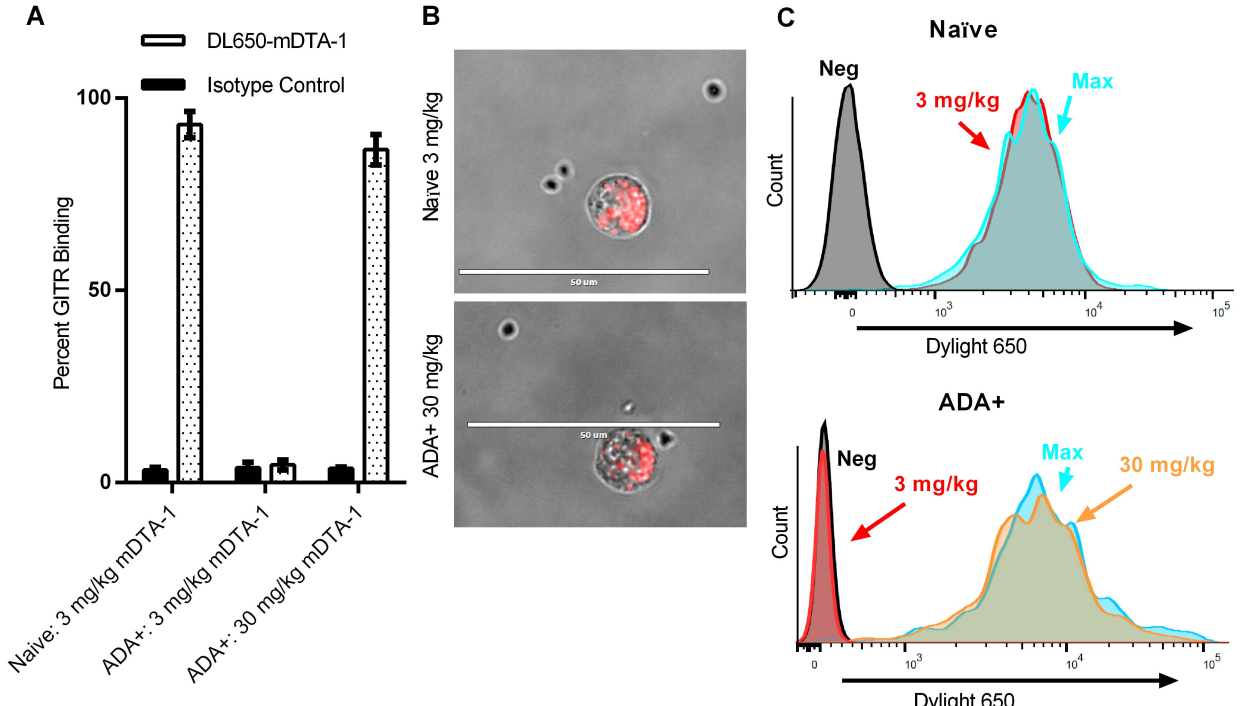
A
DL650-mDTA-1
Isotype Control
Percent GITR Binding
100
50
0
Naive: 3 mg/kg mDTA-1
ADA+: 3 mg/kg mDTA-1
ADA+: 30 mg/kg mDTA-1
B
Naive 3 mg/kg
ADA+ 30 mg/kg
50 um
50 um
C
Naïve
Neg
3 mg/kg
Max
Count
Dylight 650
ADA+
Neg
3 mg/kg
Max
30 mg/kg
Count
Dylight 650

Figure 10

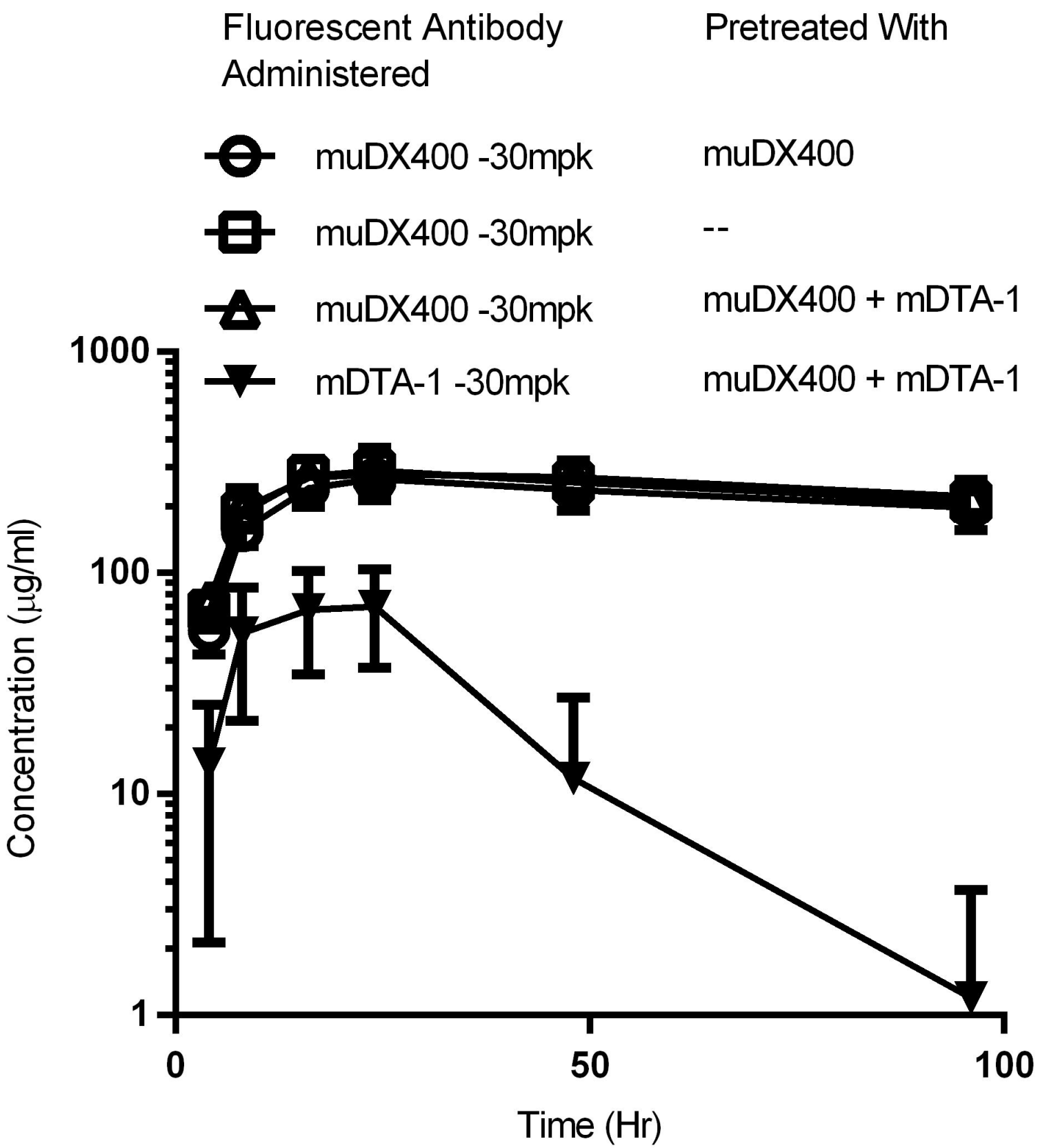
Fluorescent Antibody Administered
Pretreated With
muDX400 -30mpk
muDX400
muDX400 -30mpk
--
muDX400 -30mpk
muDX400 + mDTA-1
mDTA-1 -30mpk
muDX400 + mDTA-1
1000
100
10
1
Concentration (μg/ml)
0
50
100
Time (Hr)

Figure 11

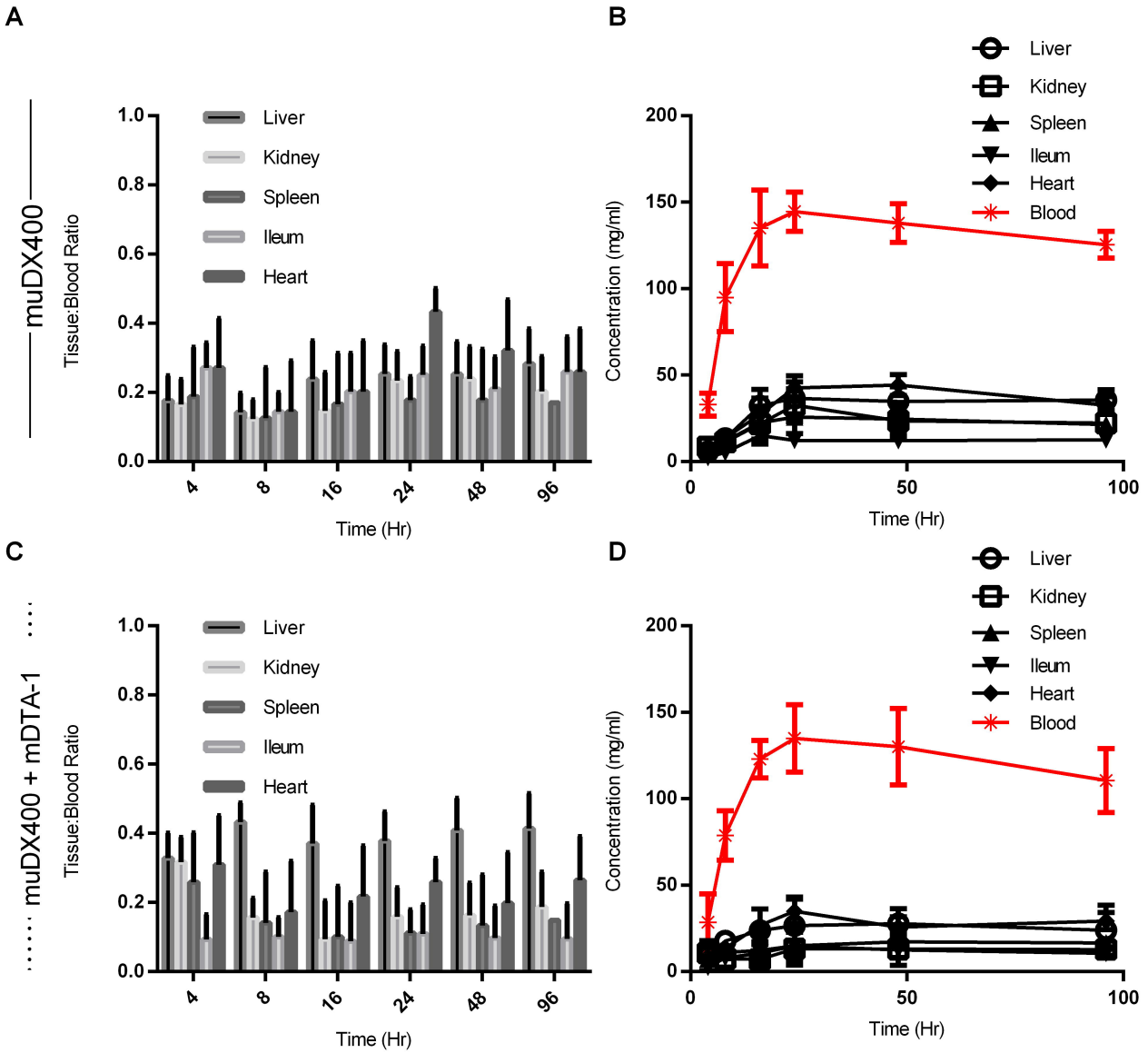
A
muDX400
Tissue:Blood Ratio
1.0
0.8
0.6
0.4
0.2
0.0
Liver
Kidney
Spleen
Ileum
Heart
4
8
16
24
48
96
Time (Hr)
B
Liver
Kidney
Spleen
Ileum
Heart
Blood
Concentration (mg/ml)
200
150
100
50
0
0
50
100
Time (Hr)
C
muDX400 + mDTA-1
Tissue:Blood Ratio
1.0
0.8
0.6
0.4
0.2
0.0
Liver
Kidney
Spleen
Ileum
Heart
4
8
16
24
48
96
Time (Hr)
D
Liver
Kidney
Spleen
Ileum
Heart
Blood
Concentration (mg/ml)
200
150
100
50
0
0
50
100
Time (Hr)